

University of Houston
Department of Mechanical Engineering
Houston, Texas 77004

NASA CR-134382

CHARACTERIZATION OF HEAT TRANSFER IN NUTRIENT MATERIALS

by

J. E. Cox R. B. Bannerot C. K. Chen L. C. Witte

Final Report, Part I

Report No. NAS-9-11676-23

31 March 1973

Reproduced by
**NATIONAL TECHNICAL
INFORMATION SERVICE**
US Department of Commerce
Springfield, VA. 22151

Sponsor: National Aeronautics and Space Administration

Contract: NAS 9-11676

Reproduction in whole or in part is permitted for any
purpose of the United States Government. Distribution
of the report is unlimited.

N74-30499

Unclass

G3/05 46869

(NASA-CR-134382) CHARACTERIZATION OF HEAT
TRANSFER IN NUTRIENT MATERIALS, PART 1
Final Report (Houston Univ.)



PRICES SUBJECT TO CHANGE

University of Houston
Department of Mechanical Engineering
Houston, Texas 77004

CHARACTERIZATION OF HEAT TRANSFER IN NUTRIENT MATERIALS

Report No. NAS 9-11676-23

31 March 1973

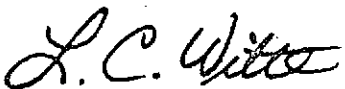
Sponsor: NASA-Manned Spacecraft Center
Houston, Texas 77058

Contract: NAS 9-11676

Technical Monitor: Dr. N. D. Heidelbaugh (DC-71)
Foods & Nutrition Branch
Preventive Medicine Division

Contract Negotiator: Mr. Louis Paletz (BC-721)
R & T Procurement Branch

Approved:



L. C. Witte, Co-Director



J. E. Cox, Director

TABLE OF CONTENTS

Nomenclature

PART I

1.0	Introduction	1
1.1	Food Heating System for Skylab	
2.0	Basic Thermal Modeling of Nutrient Materials	4
2.1	Nutrient Materials with Mixing	
2.2	Nutrient Materials without Mixing for Fixed-Temperature Boundary Conditions	
2.3	Modeling Considerations for Skylab Configuration	
3.0	Analytical Approach	12
3.1	Boundary and Initial Conditions	
3.2	General Solution	
3.3	Results for Infinite Cylinder	
3.4	Conclusions	
4.0	Finite Difference Approach	16
4.1	Introduction to Descrete Methods	
4.2	Explicit versus Implicit Models	
4.3	Finite Difference Approximations	
4.4	Application of the Finite Difference Approximations	
5.0	Basic Parametric Studies	27
5.1	Effect of Thermophysical Properties	
5.2	Effect of Heater Output	
5.3	Effect of Temperature Controls	
5.4	Effect of Initial Temperature	
5.5	Effect of Container Size	
5.6	Discussion	

References

Appendix:

- A. Adaption of Ölcer's Solution to Required Solution
- B. Computer Program Description for Analytical Solution
Discussed in Section 3.0
- C. Computer Program Description for Numerical Solution
Discussed in Section 3.0

Nomenclature

A	area
Bi	Biot number, eqn (2-6)
c	specific heat
D	domain
Fo	Fourier modulus, eqn (2-5)
h	convection coefficient
J_l	Bessel function of the first kind of order l
k	thermal conductivity
L	length of cylinder
m	mass
P	point
Q	heat transfer
Q_{tot}	total heat transfer
q	heat transfer rate
q_0	constant heat flux
R	radius of cylinder
r	radial coordinate
T	temperature
\bar{T}	average temperature
t	time
V	volume
z	axial coordinate
α	thermal diffusivity

δ Kronecker delta
 φ angular coordinate
 Φ size parameter
 ρ density

Subscripts

c center
i initial or evaluated at node i
j evaluated at node j
s surface
 ∞ surroundings

1.0 INTRODUCTION

In the processing or cooking of foods, nutrient materials are heated up to the sterilization temperature and retained at that temperature for sufficient time to destroy harmful bacteria. When foods are cooked immediately prior to serving, the nutrient material simply cools from temperatures in the sterilization region down to serving temperatures 135-150F. When foods have been processed previously and need only to be heated for serving, the nutrient material is heated from some initial temperature (whether room temperature or refrigerated temperature) up to serving temperatures. The cool, processed foods have a low level content of harmful bacteria. However, the rate of bacteria growth is accelerated in the temperature range 45-140F. Therefore, it is important in the heating process for serving to be accomplished in a reasonable time so that nutrient material does not remain in the region of accelerated bacteria growth for too long a time. For example, it is possible for bacteria to double by cell reproduction in just 20-30 minutes. Therefore, in the heating process foods cannot linger in the critical temperature range.

For the heating of foods in the ordinary, Earth-based facility, the primary mode of heat transfer is the convection mechanism, which is a very effective mechanism of heat transfer for substances having fluid characteristics. Since water boils at 212F, the surfaces of the container can be maintained at temperatures well above that of the food substances without permitting boiling of the food. The presence of large temperature differences increases the rate of heat transfer. Convection heat transfer and the presence of large temperature differences each enhance the heat transfer and reduce the time required for the heating process in the Earth-based facility.

In the space vehicle, the heating of foods is desirable for the comfort and for the psychological benefits of the crew. However,

the heat transfer is impaired by two physical factors: (a) the zero-g environment and (b) the reduced pressure level of approximately 5 psia. Since the convective mode of heat transfer depends upon bouyant forces, the zero-g environment eliminates convection; the food material must distribute energy internally by the conduction mode, which is a less effective mechanism of heat transfer. Also, at the reduced pressure level, water boils at 160F. Therefore, the temperature of the walls of the container cannot be elevated substantially above the temperature of the food material--thus, eliminating the beneficial large temperature difference.

There are then two primary tasks to be accomplished through the thermal modeling of nutrient systems: (a) prediction of the time required to heat foods to desired temperatures, and (b) development of parametric studies to optimize the system for minimum power consumption.

1.1 Food Heating System for SkyLab

The physical system for the heating of foods for SkyLab is a tray arrangement with several receptical cavities for the insertion of canned foods. The system uses two sizes of aluminum cans. The cavities are lined internally with blanket-type, electrical resistance heaters. The heaters are thermally controlled and provide a uniform heat flux of 2 watts per square inch. The sensor for the heater control system is a thermocouple, which is attached to the cavity wall.

The control system turns the heater off when the temperature sensor reaches 155F and reactivates the heater when the temperature drops to 143F. The food heating system is designed to provide hot foods at 149 ± 6 F. The aluminum cans of food receive heat on the sides and on the bottom with the top insulated. There are several different initial states of the food when inserted into the heating

system. The contents of the cans may be initially at a uniform temperature of -10F (frozen storage), 60F (ambient storage) or 130F (rehydrated). The contents of the can are pressurized to 5 psia with nitrogen. The requirements of the food heating system is that foods be heated above 140F within 132 minutes; this time requirement assures that the food passes through the microorganism growth temperature range (45-140F) rapidly enough to prevent contamination.

2.0 BASIC THERMAL MODELING OF NUTRIENT MATERIALS

The thermal analysis of the heating or cooling of nutrient materials can be considered in two parts. First, the establishment of the mechanism (or mechanisms) by which heat is transferred to (or from) the nutrient material; and second, the determination of how heat is transferred within the material itself.

The basic mechanism by which heat is transferred to (or from) the material can involve any combination of the three basic heat transfer mechanisms (conduction, convection, radiation). Heat transfer to the material by conduction involves the direct contact of two solids where contact resistance may be a consideration. Convection describes the heat transfer mechanism between a solid surface and a fluid. While thermal radiation is always present, it is particularly important in the absence of a transferring media since the other modes are non-existent. However, in order for thermal radiation to be significant, relatively large temperature differences must be present.

Two basic models are commonly involved in the analysis of the transfer of heat within the nutrient material, itself. The nutrients may be solid or plastic so that temperature gradients may be present in the material. On the other hand, the nutrient material may have sufficient fluid character so that moderate mixing occurs (whether by movement within the container or by natural convection currents). In this latter case, the temperature throughout the material is almost uniform (for moderate heating rates).

2.1 Nutrient Materials with Mixing

When a nutrient material has some fluid characteristics so that mixing may occur, the presence of internal temperature gradients are minimized, and the system can be characterized as having a uniform temperature at any instant. This basic model (illustrated in Fig. 2.1)

is known as Newtonian heating (or cooling) and is the earliest model employed in transient heat transfer analysis. At any particular instant, the nutrient system has a uniform temperature.

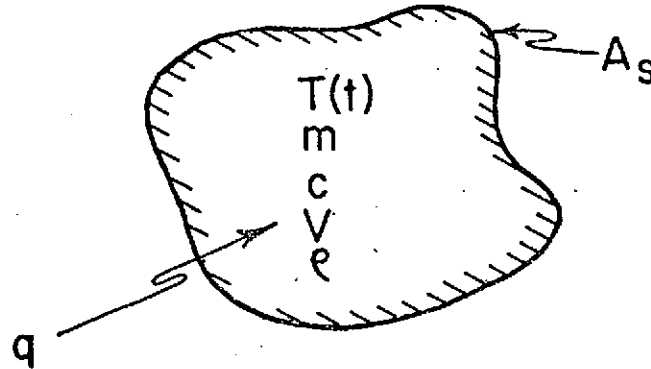


Fig. 2.1: Newtonian Heating Model

An energy balance on the system provides

$$\dot{q} = mc \frac{dT}{dt} = \rho c V \frac{dT}{dt} \quad (2-1)$$

If the heat transfer at the boundary is by convection, the heat transfer rate can be expressed in terms of the convective mechanism

$$\dot{q} = h A_s [T_\infty - T(t)] \quad (2-2)$$

If eqns (2-1) and (2-2) are combined and integrated, the temperature response of the system becomes

$$\frac{T_\infty - T(t)}{T_\infty - T_i} = e^{-\frac{h A_s}{\rho c V} \alpha t} \quad (2-3)$$

For a cylinder of radius R and length L

$$\frac{A_s}{V} = \frac{2(R/L + 1)}{R} \quad (2-4)$$

If the Fourier modulus is defined as

$$Fo = \frac{\alpha t}{R^2} \quad (2-5)$$

and the Biot number is defined as

$$Bi = \frac{hR}{k} \quad (2-6)$$

then, the dimensionless temperature response of the system can be written as

$$\frac{T_{\infty} - T(t)}{T_{\infty} - T_i} = \exp\left[-2 BiFo \left(1 + \frac{R}{L}\right)\right] \quad (2-7)$$

which is shown in Fig. 2.2.

The Newtonian model also applies to solid materials whose thermal conductivity is very large (such as silver or copper); a more accurate statement would be that the internal resistance to heat transfer by conduction is very small as compared to the surface resistance to heat transfer by convection ($Bi < 0.1$). The Newtonian model relations can be modified to include the thermal radiation mechanism; however, the ensuing integration is not straightforward.

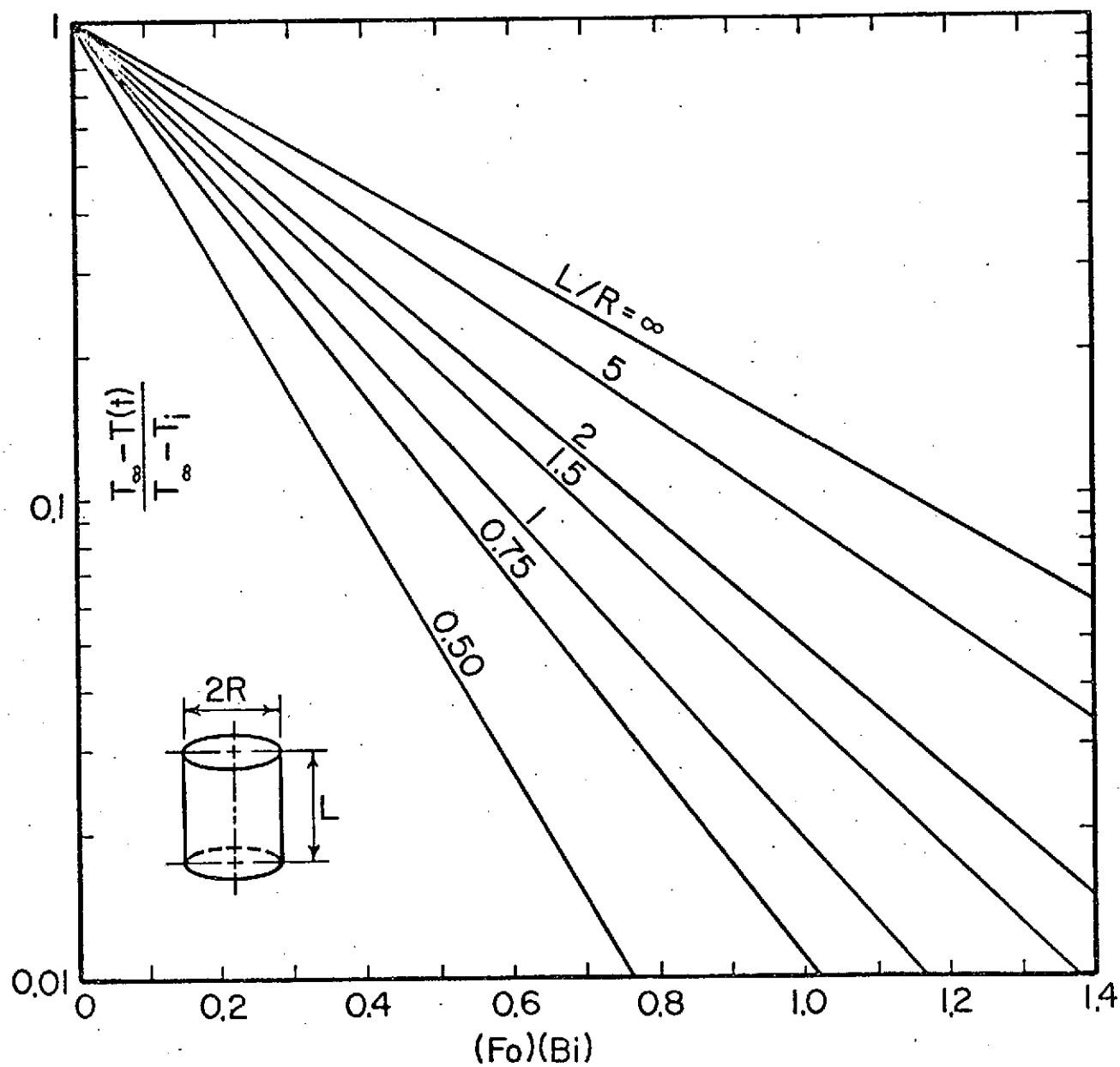
2.2 Nutrient Materials Without Mixing for Fixed-Temperature Boundary Conditions

When a nutrient material is of rigid texture (i.e., sufficiently solid to avoid mixing or convection currents), the transfer of energy internally is by the conduction mechanism. The basic partial differential equation for the axisymmetric cylindrical configuration (as shown in Fig. 2.3) may be written as

$$\frac{\partial^2 T}{\partial r^2} + \frac{1}{r} \frac{\partial T}{\partial r} + \frac{\partial^2 T}{\partial z^2} = \frac{1}{\alpha} \frac{\partial T}{\partial t} \quad (2-8)$$

for the case of constant thermophysical properties. The solution of eqn (2-8), subject to specified boundary and initial conditions, provides the local temperature distribution $T(r, z, t)$ at any instant. From the temperature distribution, the response of the average temperature of the material (or the center temperature) to a sudden change in environment at the surfaces of the finite cylinder can be established.

Fig. 2.2: Temperature Response of a Finite Cylinder for Newtonian Heating



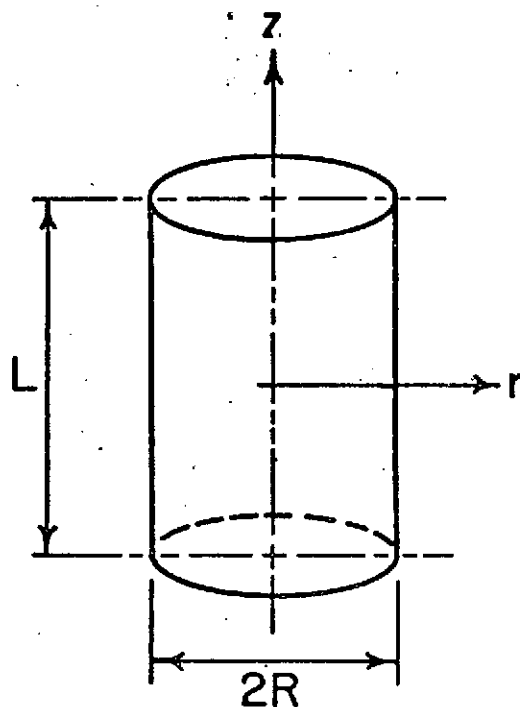


Fig. 2.3: Analytical Model of a Finite Cylinder

Analytical solutions of eqn (2-8) are available [1,2]* for basic boundary and initial conditions. For example, if the nutrient material is initially at a uniform constant temperature T_i

$$T(r, z, 0) = T_i \quad (2-9)$$

and if the surfaces of the cylinder are suddenly changed and maintained at a uniform temperature T_s

$$T(r, L/2, t) = T(r, -L/2, t) = T(R, z, t) = T_s \quad (2-10)$$

The solution of eqn (2-8) for the initial and boundary conditions (2-9) and (2-10) is

*Numbers in brackets indicate references.

$$\frac{T(r, z, t) - T_s}{T_i - T_s} = \sum_{n=1}^{\infty} \sum_{m=1}^{\infty} A_n A_m J_0\left(\mu_n \frac{r}{R}\right) \cos\left(\mu_m \frac{2z}{L}\right) \exp\left[-\left(\mu_n^2 + \mu_m^2 \frac{4R^2}{L^2}\right) Fo\right] \quad (2-11)$$

where $A_n = \frac{2}{\mu_n J_1(\mu_n)}$ and $A_m = (-1)^{m+1} \frac{2}{\mu_m}$

$$\mu_m = (2m - 1) \frac{\pi}{2} \quad \text{and} \quad J_0(\mu_n) = 0$$

The evaluation of eqn (2-11) involves the summation of a Fourier series which converges very slowly; special techniques are generally required to accelerate the convergence. From the evaluation of eqn (2-11) at a particular point, the response of the temperature of that point with time can be determined. For example, if the surfaces of a cool cylindrical container at a uniform temperature T_i were suddenly changed to a warmer temperature T_s , it would be of interest to know how fast the "cold spot" in the system responded. Equation (2-11) would then be evaluated at the centroid of the homogeneous cylinder ($r=0$, $z=0$). Fig. 2.4 shows the response of the dimensionless center temperature, T_c , with dimensionless time.

It is also of interest to know how the average temperature of the system is responding which can be obtained by

$$\bar{T}(t) = \frac{1}{V} \int_0^V T(r, z, t) dV \quad (2-12)$$

where eqn (2-11) provides the temperature expression for substitution into eqn (2-12).

$$\frac{\bar{T}(t) - T_s}{T_i - T_s} = \sum_{n=1}^{\infty} \sum_{m=1}^{\infty} \frac{4}{\mu_n^2} \frac{2}{\mu_m^2} \cdot \exp\left[-\left(\mu_n^2 + \mu_m^2 \frac{4R^2}{L^2}\right) Fo\right] \quad (2-13)$$

Fig. 2.5 shows the response of the average temperature of a cylinder in dimensionless form.

Additional information can be gained from the solution of eqn (2-11). The amount of heat transfer can be established by any

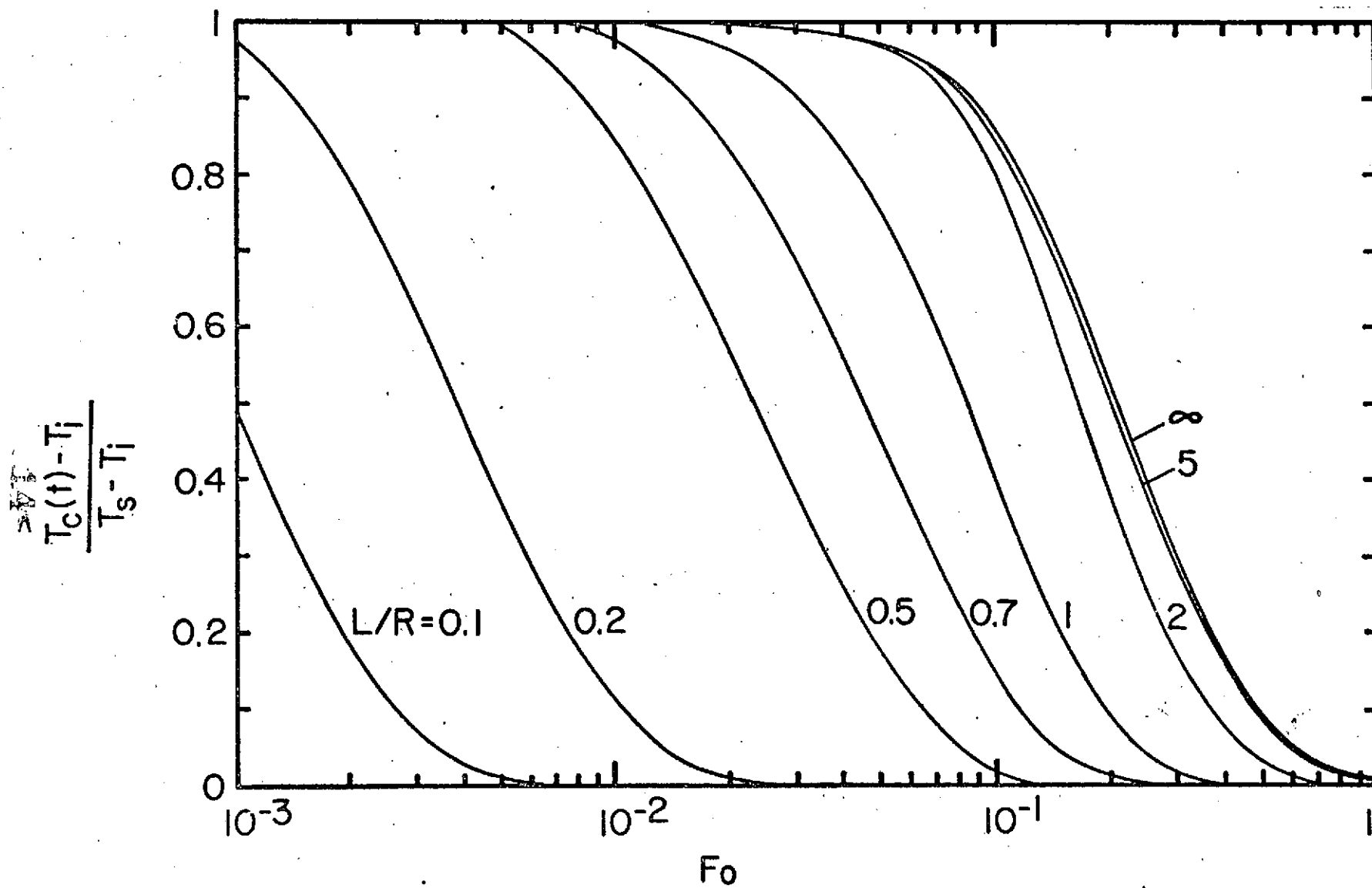


Fig. 2.4: Response of the Dimensionless Center Temperature

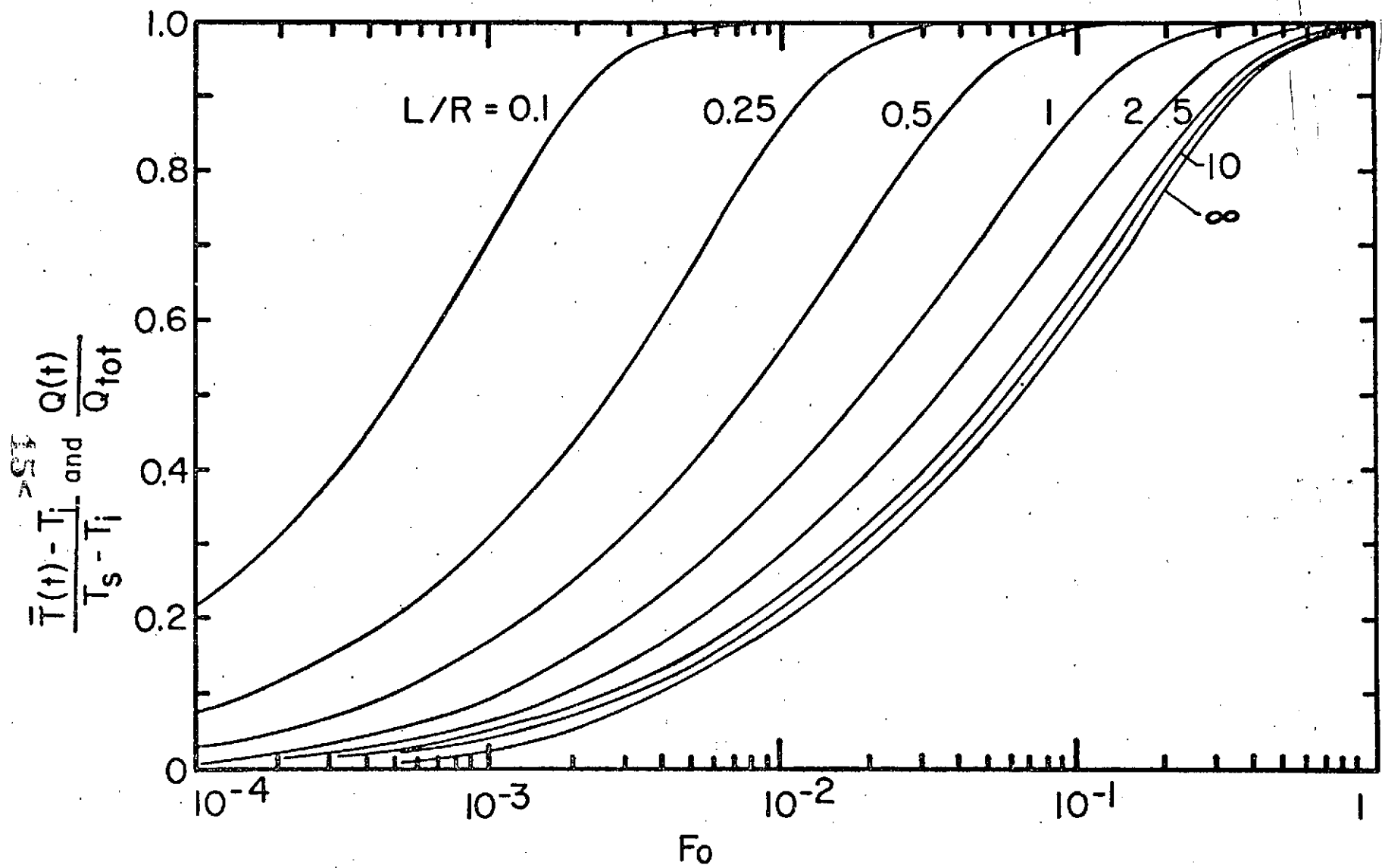


Fig. 2.5: Response of the Dimensionless Average Temperature

of several methods. Of particular interest is the fraction of the total possible heat transfer which has occurred up to any particular time. For example, if a long enough time is provided the entire system will assume the surface temperature T_s and the total heat transfer to the cylinder can easily be determined by the change in the internal energy of the cylinder, namely

$$Q_{\text{tot}} = mc(T_s - T_i) \quad (2-14)$$

The heat transfer to the cylinder from $t = 0$ to $t = t$ can be written as

$$Q(t) = mc[\bar{T}(t) - T_i] \quad (2-15)$$

The fraction of the total heat transfer transferred to the cylinder during the time interval $t = 0$ to $t = t$ can be expressed in terms of the average temperature of the cylinder

$$\frac{Q(t)}{Q_{\text{tot}}} = \frac{\bar{T}(t) - T_i}{T_s - T_i} \quad (2-16)$$

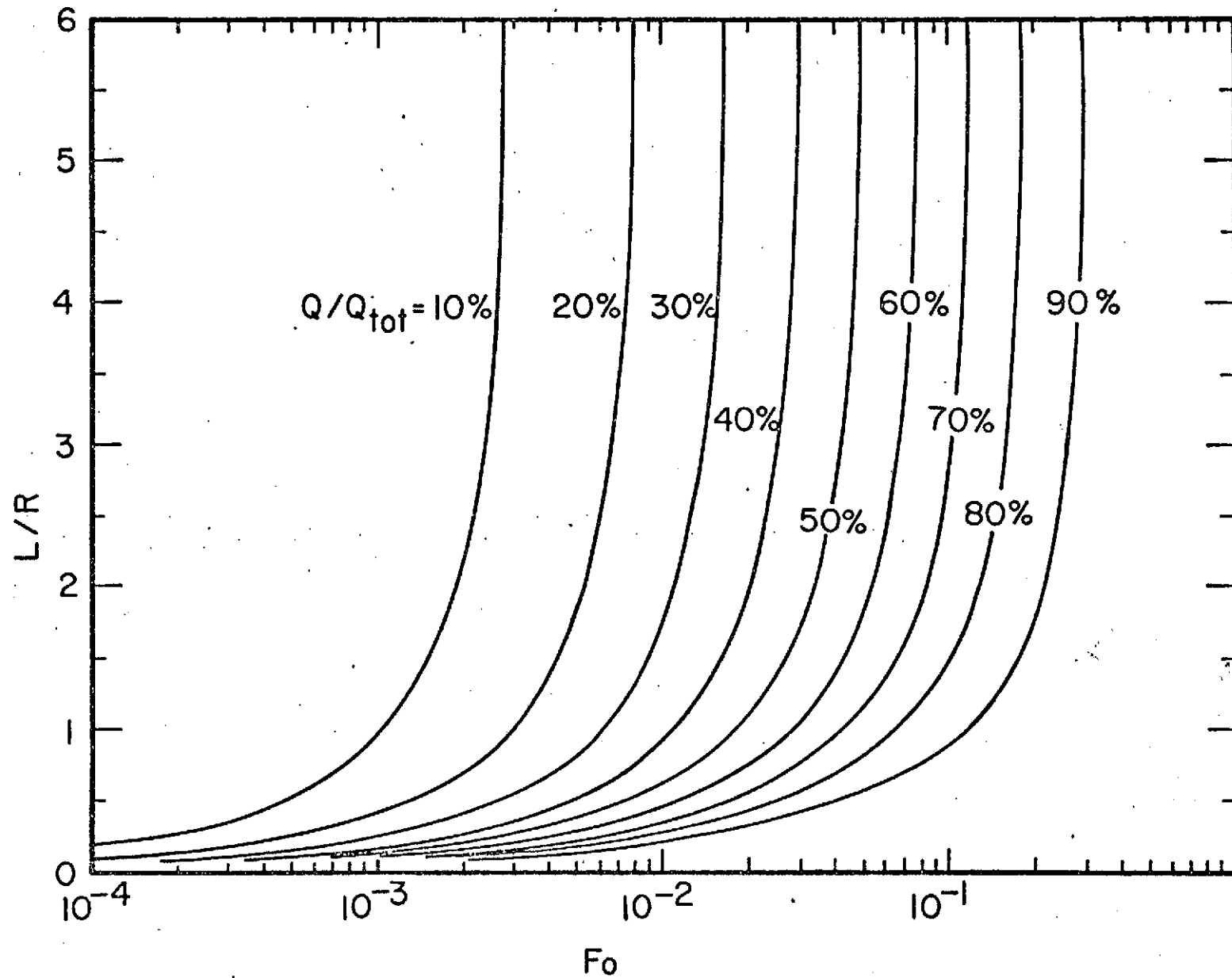
Since the right-hand side of eqn (2-16) is presented graphically in Fig. 2.5, the dimensionless heat transfer is also represented by Fig. 2.5. The fraction of the total heat transfer is also presented in different form in Fig. 2.6.

Fig. 2.2 through 2.6 present the thermal characteristics of finite cylinders for various size cylinders (i.e., for various L/R ratios). For the cases presented, the cylinder is exposed to identical conditions on each surface (i.e., the radial surface and the two ends of the cylinder). However, the results can be used for the finite cylinder, which is insulated on the ends; this case corresponds to an infinite L/R ratio where end effects are neglected.

2.3 Modeling Consideration for SkyLab Configuration

As discussed in the Introduction, the absence of buoyant forces eliminates natural convection currents in fluid-like substances. The

Fig. 2.6: Percentage of the Total Heat Transfer



distribution of heat within the nutrient material is then dependent on the conduction mode. The conduction mechanism can be adequately described by energy relationships. The two-dimensional, transient conduction equation in cylindrical coordinates was given as eqn (2-8) for the case of constant, uniform thermophysical properties. The solution of the partial differential equation for a particular application requires the establishment of appropriate initial and boundary conditions which simulate the physical situation.

There are unlimited combinations of possible boundary and initial conditions. However, the many possibilities generally can be categorized into one of three broad classifications: (a) specified surface temperature; (b) specified surface conductance; and (c) specified surface heat flux. In the preceeding section, the surface temperatures were specified; solutions associated with this type of boundary condition are usually not too difficult, but, the boundary condition does not accurately describe real-world situations. The other two classifications of boundary conditions occur more frequently in nature. The specified surface conductance describes the interaction of a fluid and a solid surface through the convection mechanism. Although the surface conductance (or convection coefficient) is assumed constant, the heat transfer rate is not if there is a change in the temperature of the solid surface and/or the fluid. The third classification of boundary conditions is the specified surface heat flux, which accurately describe situations involving electrical heating elements, such as in the SkyLab system. In the SkyLab configuration, a uniform heat flux acts on the sides and bottom of the container with the top insulated. In order to simulate the SkyLab system, the model must be capable of describing intermittent heating periods.

Due to the presence of zero-g conditions, the boundary conditions may be complicated somewhat. If the nutrient material fails

to "wet" the surface of the container, the food may "float" in a partially filled container. The situation may occur where the food separates from the heating surface. The nitrogen gas filling the voids surrounding the nutrient material has a very low thermal conductivity and acts as an insulator between the heating surface and the nutrient material. In this situation, thermal radiation may be the predominate mechanism to be considered. Since the temperature of the heating surface is only $149 \pm 6^\circ\text{F}$, the radiation mechanism is not an effective mode of heat transfer. Since heat is not effectively transferred to the food, the heater is only heating the wall of the can. When its temperature exceeds the cutoff, the heater is deactivated. The heater will in fact be off most of the time, and the heating time will be extended substantially.

In modeling food substances, the nature of the nutrient materials themselves is an important consideration. Foods have heterogeneous character (i.e., a non-uniform composition such as soups, stew, etc.). It is standard practice in modeling such systems to establish some "weighted" average values of the thermophysical properties for the various food components and then to treat the material as homogeneous in nature. In the zero-g environment, the nutrient material may form internal voids or cavities which may be filled with gas. The presence of voids in the material may effect the internal heat transfer substantially (as compared to the heterogeneous characteristics of several food substances) because of the insulating effect of such cavities. The available data concerning the thermophysical properties of nutrient materials are somewhat limited. The data are scattered in many diverse sources in the literature. Also, in gathering data from the literature, one questions the validity of some of the data because of the experimental techniques employed in the measurements.

3.0 ANALYTICAL APPROACH

3.1 Boundary and Initial Conditions

For the model illustrated in Fig. 2.3, the conduction relation for the heating of nutrient materials was given in eqn (2-8) for the case of constant thermophysical properties. To solve this relation, appropriate initial and boundary conditions must be selected which best describe the physical configuration of the Skylab system. If the nutrient material is initially at a constant, uniform temperature, the initial condition becomes

$$T(r, z, 0) = T_i. \quad (3-1)$$

The boundary condition for the insulated top is

$$\frac{\partial T(r, L/2, t)}{\partial z} = 0. \quad (3-2)$$

For the intermittent heating of the sides and bottom, the appropriate boundary conditions can be written as

$$\frac{\partial T(R, z, t)}{\partial r} = \frac{\partial T(r, -L/2, t)}{\partial z} = \begin{cases} \frac{q_0}{k} & \text{(constant heat flux; heater on)} \\ 0 & \text{(insulated; heater off)} \end{cases} \quad (3-3)$$

Along with the physical boundary conditions is the stipulation that the temperature remain finite along the axis of the cylinder.

3.2 General Solution

There is no single analytical solution which will satisfy all these conditions simultaneously. However, a piece-wise solution can be formed by adding together a series of solutions, each valid for a short time increment (e.g., one heating period). There are actually only two different solutions required. One for the time when the heater is on, and the other for when the heater is off (which is really a special case of the first with $q_0 = 0$).

Ölcer [3] developed a general solution (additional details in Appendix A). For a flux, q_0 , applied at the radial and bottom surfaces, insulated top, and an arbitrary initial temperature distribution, $T(r, z, 0) = T_i(r, z)$ (For the second and succeeding heating periods, the initial temperature is non-uniform.), the transient axisymmetric temperature response is:

$$\begin{aligned}
 T(r, z, t) = & \frac{2}{R^2 L} \int_0^R \int_{-\frac{L}{2}}^{\frac{L}{2}} T_i(r, z) r dr dz + \left[\frac{\alpha t}{kL} + \frac{2\alpha t}{kR} \right] \{q_0\} \\
 & + \left[\frac{2}{kL} \left(\frac{\left(\frac{L}{2} - z\right)^2}{4} - \frac{L^2}{12} \right) + \frac{R}{2k} \left(\frac{r^2}{R^2} - \frac{1}{2} \right) \right] \{q_0\} \\
 & + \frac{16\pi}{R^2 L} \sum_{m=0}^{\infty} \sum_{n=0}^{\infty} \frac{J_0(\mu_m r) \cos \left[\frac{n\pi}{2} + \frac{n\pi z}{L} \right] \exp(-\alpha \lambda_{mn}^2 t)}{2(1 + \delta_{no}) J_0^2(\mu_m R)} \\
 & \left[\int_{-\frac{L}{2}}^{\frac{L}{2}} \int_0^R J_0(\mu_m r) \cos \left(\frac{n\pi}{2} + \frac{n\pi z}{L} \right) T_i(r, z) r dr dz \right. \\
 & \left. - \frac{R}{k \lambda_{mn} \mu_m} J_1(\mu_m R) \{q_0\} \right] \quad (3-4)
 \end{aligned}$$

where $\{q_0\}$ indicates the two cases of heater on and off

$$\lambda_{mn}^2 = \mu_m^2 + \left(\frac{n\pi}{L} \right)^2 \quad (3-5)$$

where $\mu_m R \geq 0$ is the m th root of

$$J_0'(\mu_m R) = 0 \quad (3-6)$$

and the prime (') denotes differentiation with respect to the argument.

For the first heating period the initial temperature is uniform and

$$T_i(r, z) = T_i \quad (3-7)$$

so that the first integral becomes equal to T_i , and the other integration involving T_i vanishes.

For a given initial temperature distribution and surface heat flux, eqn (3-4) can be used to calculate the local temperature within the cylinder, $T(r, z, t)$. The highest temperature will be at the bottom corner, point $(R, 0)$. Therefore, the temperature $T(R, 0, t)$ is monitored until it reaches the predetermined maximum value. At this time, t_1 , the entire temperature distribution, $T(r, z, t_1)$, is evaluated; this temperature distribution becomes $T_i(r, z)$ for the second phase of the first heating cycle. With $q_0 = 0$ (heater off) eqn (3-4) is used to determine the temperature within the food. When the monitored temperature at the bottom corner $(R, 0)$ drops to the predetermined minimum value, the heater is again activated. The temperature distribution at this time becomes the initial condition for the first phase of the second heating cycle. Equation (3-4) with non-zero boundary heat flux is used to determine the temperature. This procedure is continued until the food is heated to the desired level. The average food temperature can be determined either by averaging the temperature distribution:

$$\bar{T}(t) = \frac{2}{R^2 L} \int_{-\frac{L}{2}}^{\frac{L}{2}} \int_0^R T(r, z, t) r dr dz \quad (3-8)$$

or by dividing the total heat added to the food by the heat capacity of the food. Hence

$$\bar{T}(t) = \frac{q_0 (2\pi RL + \pi R^2) t_{on}}{c} \quad (3-9)$$

where t_{on} is the total "on-time" for the heater.

3 Results for an Infinite Cylinder

The analytical method outlined above has been programed and run for the special case of an infinite cylinder ($n = 0$, $L \rightarrow \infty$) heated on the cylindrical surfaces only [4]. An infinitely long cylinder is equivalent to a finite cylinder insulated on both ends. A discussion of the program and a simplified flow chart appear in Appendix B.

Figure 3.1 depicts typical temperature distributions as a function of non-dimensional radius, r/R (with heater at $142 \pm 8^\circ\text{F}$). Curve 3 represents the distribution when the wall temperature first reaches T_{max} (i.e., the end of the first heating phase). Curves 1 and 2 are the distributions at one-third and at two thirds of the total heating time of the first phase. The remaining odd numbered curves indicate the distributions at the end of each successive heating phase. The even numbered curves indicate the distributions at end of the successive insulated phases (i.e., just before the heater is reactivated).

3.4 Conclusions

While satisfactory results were obtained with the analytical model, it was decided not to be continued to the finite cylinder case for the following reasons:

1. A discontinuity always exists when switching from one solution to the other due to the discontinuous manner in which the flux is switched on and off. The effect of this discontinuity is minor.
2. Considerable computation time is necessary and the time required will increase considerably by the inclusion of the double summation required for the finite cylinder.
3. A finite difference model appeared more attractive. Computation time was reduced and the finite difference model is more versatile. The inclusion of different boundary conditions and a study of heterogeneous effects are reasonable extensions.

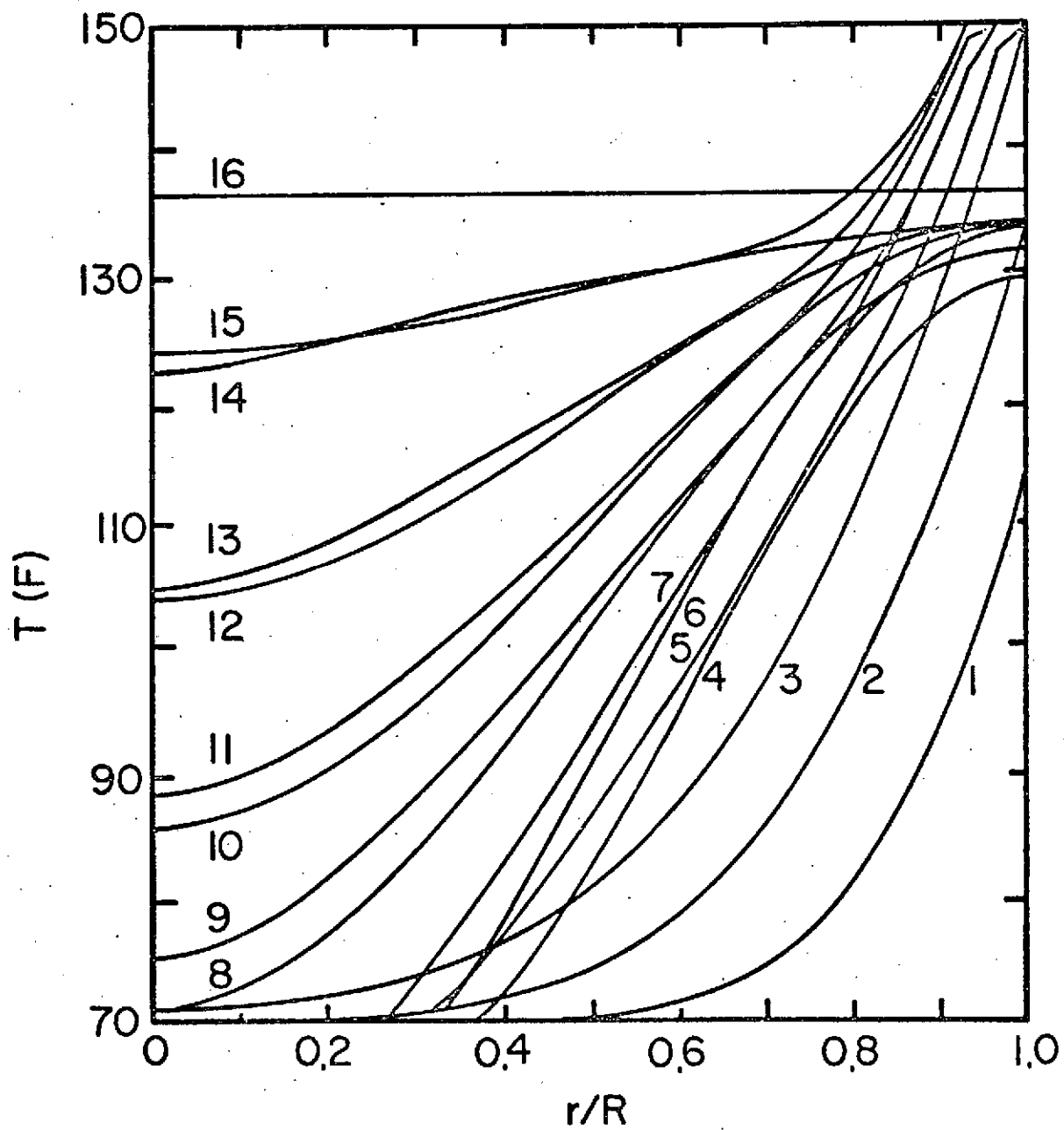


Fig. 3.1: Temperature Distribution at the Conclusion of the Heating (Odd Numbers) and Insulated (Even Numbers) Phases in the Infinite Cylinder

4.0 FINITE DIFFERENCE APPROACH

4.1 Introduction to Discrete Methods

The ultimate goal of discrete methods is the reduction of a continuous system to an equivalent lumped-parameter system which is suitable for solution on a digital computer. The basic approximation involves the replacement of a continuous domain D by a matrix of discrete points (nodes) within D , as shown in Fig. 4.1 for two dimensions.

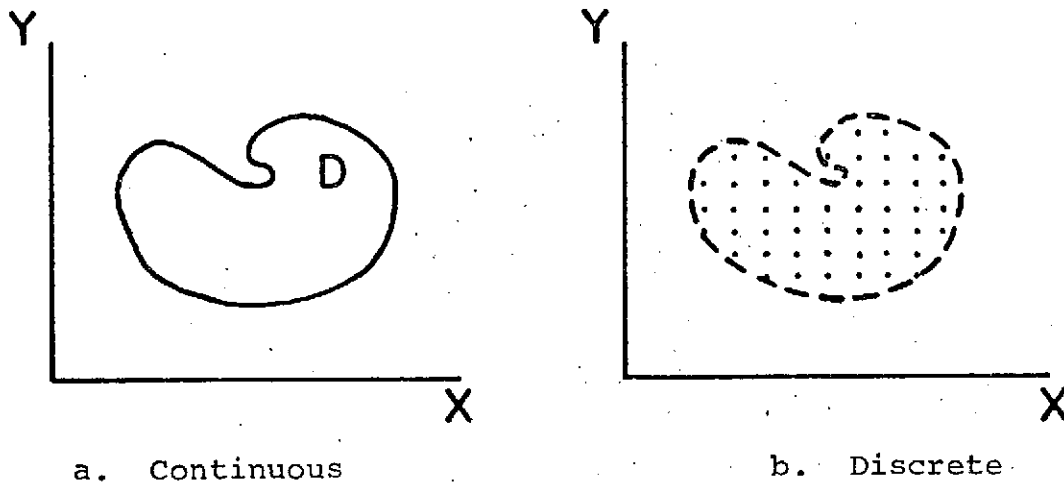


Fig. 4.1. Discrete Approximation of a Continuous Two-Dimensional Domain

Instead of developing a solution defined everywhere in D , only approximations are obtained at isolated points (nodes), $P_{i,j}$. Intermediate values, integrals, and derivatives may be obtained from this discrete solution by interpolation. This mathematical discretization replaces the derivatives by discrete approximations, (e.g., finite difference approximations).

At a given node, at a given time, the values of the coordinates define a unique location. For an axisymmetric cylindrical coordinate system, the set $(r_i, z_j, t^{(n)})$ define such a location where r_i is the

radial coordinate, z_j is the axial coordinate, and $t^{(n)}$ is the time after n time steps. Hence the dependent variable (temperature in this case) at this point is

$$T = T(r_i, z_j, t^{(n)}) = T_{i,j}^{(n)}. \quad (4-1)$$

At a given time, the nodes (r_i, z_j) , (r_{i-1}, z_j) , (r_i, z_{j-1}) and (r_{i-1}, z_{j-1}) define a subregion in the shape of an annulus of inner radius r_{i-1} , outer radius r_i , and thickness $z_i - z_{i-1}$ as depicted in Fig. 4.2.

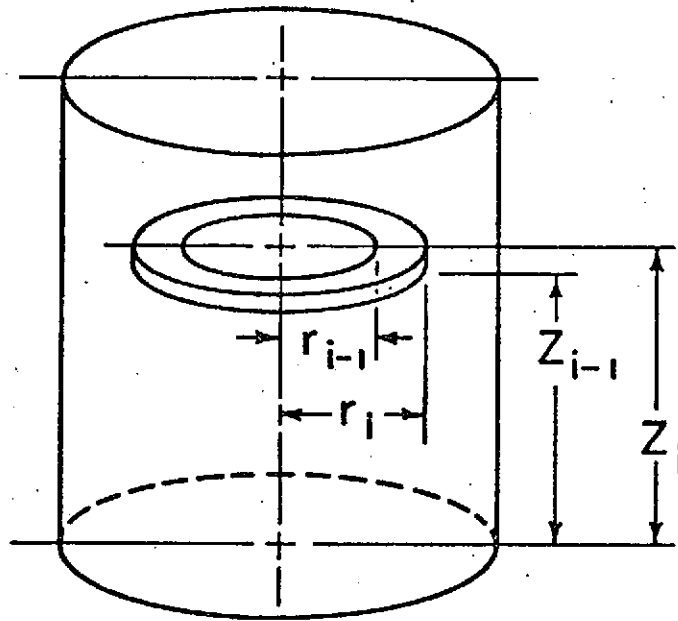


Fig. 4.2. Subregion Formed by Nodes (r_i, z_j) , (r_{i-1}, z_j) , (r_i, z_{j-1}) , and (r_{i-1}, z_{j-1})

4.2 Explicit versus Implicit Models

The standard finite difference approximations for partial derivatives can be found in most applied mathematics texts [5,6,7] and are

dealt with in more detail in the next section. In general, there are two techniques available for approximating the differential equation in the transient problem. These are the implicit and explicit methods.

In the explicit technique, the future temperature at some node (i,j) is expressed in terms of its present temperature and that of surrounding nodes; that is, (for a first order approximation)

$$T_{i,j}^{(n+1)} = f(T_{i,j-1}^{(n)}, T_{i,j+1}^{(n)}, T_{i+1,j}^{(n)}, T_{i-1,j}^{(n)}, T_{i,j}^{(n)}) \quad (4-2)$$

where the form of the functional relationship depends on the governing differential equation. Since the initial temperature distribution is known, this technique can be used successively at each node to advance the solution one time step (i.e., eqn (4-2) is applied k times if there are k nodes). The process can be repeated indefinitely until the required time has elapsed. The accuracy of the solution depends largely on the spatial nodal spacing. The closer the nodes, (hence, a larger number of nodes for a given physical system) the more nearly accurate the approximation. The fundamental limitation of the explicit representation is that for a given nodal spacing the maximum rate at which the solution can be propagated (in time) is set. (If this rate is exceeded the solution becomes unstable). In general, the more sparse the nodes, the smaller the maximum allowable time step ($t^{(n+1)} - t^{(n)} = \Delta t$) becomes. This can be a severe limitation to the explicit method for a given application. To increase the maximum Δt requires more nodes, which in turn requires additional computation at each time step. Thus, even though fewer time steps may be needed, each one becomes more tedious. General rules have been developed for the maximum time step allowable under various conditions [8].

The implicit technique removes the possibility of this instability at the expense of increased computational complexity. In the implicit technique, the future temperatures at a given node (i,j) and the

surrounding nodes are expressed in terms of the present temperature of node (i,j); that is, (for a first order approximation)

$$f(T_{i,j-1}^{(n+1)}, T_{i,j+1}^{(n+1)}, T_{i-1,j}^{(n+1)}, T_{i+1,j}^{(n+1)}, T_{i,j}^{(n+1)}) = T_{i,j}^{(n)} \quad (4-3)$$

where again the functional form of f depends on the specific problem. This relationship must be determined at each node leading to a set of simultaneous, linear algebraic equations to be solved at each time step. This method is unconditionally stable in time but, of course, can introduce large round-off errors if the time step is excessive. Again it is noted that while the implicit method seems more attractive because of its stability characteristic, the requirement in the implicit model of solving a set (one equation for each node) of simultaneous equation can hardly be compared to the solution of a set of independent equations required in the explicit model.

4.3 Finite Difference Approximations

The following are the finite difference approximations required

$$\left. \frac{\partial T}{\partial r} \right|_{i,j} \cong \frac{T_{i+1,j}^{(n)} - T_{i-1,j}^{(n)}}{r_{i+1} - r_{i-1}} \quad (4-4) \quad \begin{array}{l} \text{Central difference} \\ \text{approximation of} \\ \text{the first derivative} \end{array}$$

$$\left. \frac{\partial^2 T}{\partial r^2} \right|_{i,j} \cong \frac{T_{i+1,j}^{(n)} - 2T_{i,j}^{(n)} + T_{i-1,j}^{(n)}}{\left(\frac{r_{i+1} - r_{i-1}}{2} \right)^2} \quad (4-5) \quad \begin{array}{l} \text{Central difference} \\ \text{approximation for the} \\ \text{second derivative} \end{array}$$

$$\left. \frac{\partial T}{\partial t} \right|_{i,j} \cong \frac{T_{i,j}^{(n+1)} - T_{i,j}^{(n)}}{t_{i+1} - t_i} \quad (4-6) \quad \begin{array}{l} \text{The forward difference} \\ \text{approximation for the} \\ \text{first derivative} \end{array}$$

The other required approximation follows.

Due to the complexity of the implicit model, it was decided to use an explicit model for the problem first. The explicit finite difference approximation for eqn (2-8) around the node (i,j) is:

$$\begin{aligned}
& \frac{T_{i+1,j}^{(n)} - 2T_{i,j}^{(n)} + T_{i-1,j}^{(n)}}{\left(\frac{r_{i+1} - r_{i-1}}{2}\right)^2} + \frac{1}{r_i} \frac{T_{i+1,j}^{(n)} - T_{i-1,j}^{(n)}}{r_{i+1} - r_{i-1}} \\
& + \frac{T_{i,j+1}^{(n)} - 2T_{i,j}^{(n)} + T_{i,j-1}^{(n)}}{\left(\frac{z_{j+1} - z_{j-1}}{2}\right)^2} = \frac{1}{\alpha} \frac{T_{i,j}^{(n+1)} - T_{i,j}^{(n)}}{t^{(n+1)} - t^{(n)}}. \quad (4-7)
\end{aligned}$$

Equation (4-7) applies for any nodal spacing. However, it is convenient at this time to assign a uniform nodal network. At each z_j there are N radial nodes. Node 1 is on the center line of the cylinder; node N is on the circumferential surface. The nodes are equally spaced; i.e.,

$$\Delta r = \frac{R}{N - 1}. \quad (4-8)$$

There are M equally spaced nodes in the z direction. Hence,

$$\Delta z = \frac{L}{M - 1}. \quad (4-9)$$

The time steps are also of equal length and are denoted Δt . With the nodal matrix thus defined eqn (4-7) becomes

$$\begin{aligned}
& \frac{T_{i+1,j}^{(n)} - 2T_{i,j}^{(n)} + T_{i-1,j}^{(n)}}{(\Delta r)^2} + \frac{1}{(i-1)(\Delta r)} \frac{T_{i+1,j}^{(n)} - T_{i-1,j}^{(n)}}{2(\Delta r)} \\
& + \frac{T_{i,j+1}^{(n)} - 2T_{i,j}^{(n)} + T_{i,j-1}^{(n)}}{(\Delta z)^2} = \frac{1}{\alpha} \frac{T_{i,j}^{(n+1)} - T_{i,j}^{(n)}}{(\Delta t)}. \quad (4-10)
\end{aligned}$$

The required temperature is $T_{i,j}^{(n+1)}$. From eqn (4-10)

$$\begin{aligned}
T_{i,j}^{(n+1)} &= T_{i+1,j}^{(n)} \alpha(\Delta t) \left[\frac{1}{(\Delta r)^2} + \frac{1}{2(i-1)(\Delta r)^2} \right] \\
&+ T_{i,j}^{(n)} \left[1 - 2\alpha(\Delta t) \left(\frac{1}{(\Delta r)^2} + \frac{1}{(\Delta z)^2} \right) \right] \\
&+ T_{i-1,j}^{(n)} \alpha(\Delta t) \left[\frac{1}{(\Delta r)^2} - \frac{1}{2(i-1)(\Delta r)^2} \right] \\
&+ \frac{\alpha(\Delta t)}{(\Delta z)^2} T_{i,j+1}^{(n)} + \frac{\alpha(\Delta t)}{(\Delta z)^2} T_{i,j-1}^{(n)}. \quad (4-11)
\end{aligned}$$

If

$$\frac{\alpha(\Delta t)}{(\Delta r)^2} = M_r$$

$$\frac{\alpha(\Delta t)}{(\Delta z)^2} = M_z$$

then

$$\frac{\alpha(\Delta t)}{2(i-1)(\Delta r)^2} = \frac{M_r}{2(i-1)}$$

and eqn (4-11) becomes

$$\begin{aligned} T_{i,j}^{(n+1)} = & T_{i+1,j}^{(n)} \left[\frac{2i-1}{2(i-1)} \right] M_r + T_{i,j}^{(n)} \left[1 - 2M_r - 2M_z \right] \\ & + T_{i-1,j}^{(n)} \left[\frac{2i-3}{2(i-1)} \right] M_r + T_{i,j+1}^{(n)} M_z + T_{i,j-1}^{(n)} M_z \end{aligned} \quad (4-12)$$

Equation (4-12) is the general form of the algorithm required to generate the temperature at all interior points (i.e., those not directly effected by the boundary).

At the center line, $i = 1$ and the coefficients of $T_{i\pm 1,j}^{(n)}$ become infinite in eqn (4-12). However, by symmetry

$$T_{2,j}^{(n)} = T_{-2,j}^{(n)} \quad (4-13)$$

so that for $1 < j < M$

$$\begin{aligned} T_{1,j}^{(n+1)} = & T_{1,j}^{(n)} \left[1 - 2M_r - 2M_z \right] + T_{2,j}^{(n)} 2M_r \\ & + T_{i,j}^{(n)} M_z + T_{1,j-1}^{(n)} M_z \end{aligned} \quad (4-14)$$

At the outer radius for a constant heat flux boundary condition

$$k \frac{\partial T}{\partial r} \Big|_{r=R} = q_0 \quad (4-15)$$

The finite difference approximation to eqn (4-15) is (at $i=N$)

$$\frac{T_{N+1,j}^{(n)} - T_{N-1,j}^{(n)}}{2(\Delta r)} = \frac{q_0}{k}$$

or

$$T_{N+1,j}^{(n)} = T_{N-1,j}^{(n)} + \frac{q_0}{k} 2(\Delta r). \quad (4-16)$$

Substitution of eqn (4-16) into eqn (4-12) yields for $1 < j < M$

$$\begin{aligned} T_{N,j}^{(n+1)} = & 2M_r T_{N-1,j}^{(n)} + [1 - 2M_r - 2M_z] T_{N,j}^{(n)} \\ & + M_z [T_{N,j+1}^{(n)} + T_{N,j-1}^{(n)}] + \frac{2N-1}{2(N-1)} \frac{2(\Delta r)q_0}{k} M_r. \end{aligned} \quad (4-17)$$

At the top surface

$$\left. \frac{\partial T}{\partial z} \right|_{z=L/2} = 0. \quad (4-18)$$

The finite difference approximation to eqn (4-18) is: (at $j=M$)

$$T_{i,M+1}^{(n)} - T_{i,M-1}^{(n)} = 0$$

or

$$T_{i,M+1}^{(n)} = T_{i,M-1}^{(n)}. \quad (4-19)$$

Substitution of eqn (4-19) into eqn (4-12) yields for $1 < i < N$

$$\begin{aligned} T_{i,M}^{(n+1)} = & \frac{2i-1}{2(i-1)} M_r T_{i+1,M}^{(n)} + [1 - 2M_r - 2M_z] T_{i,M}^{(n)} \\ & + \frac{2i-3}{2(i-1)} M_r T_{i-1,M}^{(n)} + 2M_z T_{i,M-1}^{(n)}. \end{aligned} \quad (4-20)$$

At the bottom surface

$$k \left. \frac{\partial T}{\partial z} \right|_{z=-L/2} = q_0 \quad (4-21)$$

or

$$\frac{T_{i,0}^{(n)} - T_{i,z}^{(n)}}{2(\Delta z)} = \frac{q_0}{k}$$

and

$$T_{i,0}^{(n)} = T_{i,2}^{(n)} + \frac{q_0 2(\Delta z)}{k} \quad (4-22)$$

The solution at the bottom surface becomes for $1 < i < N$

$$\begin{aligned} T_{i,1}^{(n+1)} &= \frac{2i-1}{2(i-1)} M_r T_{i+1,1}^{(n)} + \left[1 - 2M_r - 2M_z \right] T_{i,1}^{(n)} \\ &+ \frac{2i-3}{2(i-1)} M_r T_{i-1,1}^{(n)} + 2M_z T_{i,z}^{(n)} \\ &+ M_z \frac{2(\Delta z)}{k} q_0 \end{aligned} \quad (4-23)$$

At the top edge, $i = N$ and $j = M$ so that from eqn (4-17) and (4-19)

$$\begin{aligned} T_{N,M}^{(n+1)} &= 2M_r T_{N-1,M}^{(n)} + \left[1 - 2M_r - 2M_z \right] T_{N,M}^{(n)} \\ &+ 2M_z T_{N,M-1}^{(n)} + \frac{2N-1}{2(N-1)} M_r \frac{2(\Delta r)}{k} q_0 \end{aligned} \quad (4-24)$$

At the bottom edge $i = N$ and $j = 1$ so that from eqn (4-17) and (4-22)

$$\begin{aligned} T_{N,1}^{(n+1)} &= 2M_r T_{N-1}^{(n)} + \left[1 - 2M_r - 2M_z \right] T_{N,1}^{(n)} \\ &+ 2M_z T_{N,2}^{(n)} + \frac{2N-1}{2(N-1)} M_r \frac{2(\Delta r)}{k} q_0 \\ &+ M_z \frac{2(\Delta z)}{k} q_0 \end{aligned} \quad (4-25)$$

At the bottom center $T_{0,1} = T_{2,1}$ and from eqn (4-23)

$$T_{1,1}^{(n+1)} = 2M_r T_{2,1}^{(n)} + \left[1 - 2M_r - 2M_z \right] T_{1,1}^{(n)} + 2M_z T_{1,2}^{(n)} + \frac{2(\Delta z)}{k} M_z q_o \quad (4-26)$$

At the top center $T_{0,N} = T_{2,N}$ and from eqn (4-20)

$$T_{1,N}^{(n+1)} = 2M_r T_{2,N}^{(n)} + \left[1 - 2M_r - 2M_z \right] T_{1,N}^{(n)} + 2M_z T_{1,N-1}^{(n)} \quad (4-27)$$

4.4 Application of the Finite Difference Approximations

A thirty-six node model (6 radial & 6 axial nodes) was selected for the homogeneous cylinder. Equations (4-12), (4-14), (4-17), (4-20), (4-23), (4-24), (4-25), (4-26) and (4-27) were used in a Fortran IV G program. A simplified flow chart appears in Appendix C.

A simplified analysis [8] was made to determine the maximum propagation speed of the solution. From eqn (4-12) it is apparent that if the term

$$1 - 2M_r - 2M_z$$

is negative, then the larger $T_{i,j}^{(n)}$, the smaller $T_{i,j}^{(n+1)}$. This result is physically unreasonable. Therefore, time increments must be restricted such that

$$1 - 2M_r - 2M_z > 0$$

$$1 - \frac{2\alpha(\Delta t)}{(\Delta r)^2} - \frac{2\alpha(\Delta t)}{(\Delta z)^2} > 0$$

$$\frac{1}{(\Delta r)^2} + \frac{1}{(\Delta z)^2} < \frac{1}{2\alpha(\Delta t)} \quad (4-28)$$

For the can sizes expected on Skylab ($R < 2$ inches, $L < 4$ inches), with a thermal diffusivity of water ($\alpha \approx 5 \times 10^{-3}$ ft²/hr) and for the nodal network assumed ($\Delta r = \frac{R}{5}$, $\Delta z = \frac{L}{5}$), the restriction in eqn (4-28) becomes

$$\frac{25}{R^2} + \frac{25}{L^2} < \frac{1}{10^{-2}(\Delta t)}$$

$$\frac{25}{1/36} + \frac{25}{1/9} < \frac{100}{(\Delta t)}$$

or

$$\Delta t < \frac{100}{25(36) + 9(25)} = .089 \text{ hr} \sim 5 \text{ minutes}$$

Hence the time steps cannot exceed 5 minutes each. From experimental evidence, it is known that as the can approaches its maximum temperature, the heating phase of heater cycle may be as short as a few seconds. If the model is to be capable of simulating this heating period, the time step should be on the order of a second. Since the time steps required are well below the maximum allowable, the explicit model will be sufficient.

The predictions of the finite-difference model can be demonstrated by looking at the graphical presentations in Fig. 4.3, 4.4 and 4.5. The temperature specification for the heated food is 149±6F. Therefore, the thermal control on the uniform heat flux heater are specified accordingly. When the hottest point on the heating surfaces reaches 155F, the heater is deactivated and the food stuffs are treated as an adiabatic system (i.e., no heat losses); when the hottest spot on the surface has dropped to 143F, the heater is reactivated, and the cycle continues until the average temperature of the food reaches 149F. In each of the cases shown, the food was assumed to have thermal diffusivity of water and a uniform surface heat flux of 2.0 watts per square inch was employed. In each of the figures, two temperatures

are shown - the average temperature of the food and the temperature of the coldest internal point.

The temperature responses of the small container and the large container are shown in Fig. 4.3 and 4.4, respectively. Two initial temperature conditions ($T_i = 130\text{F}$ and $T_i = 60\text{F}$) are presented in each figure. This same model was employed in evaluating the temperature responses for an initial temperature of -10F and the results are shown for both container sizes in Fig. 4.5. It should be carefully noted that this particular model did not have the capacity for including the latent energy associated with the phase change in the thawing process. If the nutrient materials were similar to water, the latent heat of fusion (or melting) is 79.7 calories per gram (143 BTU/lbm). If the melting process were approximated by a "lumped" parameter (i.e., assuming that there are no temperature gradients present in the nutrient material during the melting process), the additional time required would be

0.30 hours (small container)

0.39 hours (large container)

The finite-difference model can be modified to include the latent energy of thawing to provide more accurate predictions of the required heating times.

The basic finite-difference model has a number of input parameters. Each of these parameters can be investigated individually to determine its influence on the temperature response of the nutrient material.

5.0 BASIC PARAMETRIC STUDIES

The heat transfer analysis provides the vehicle for performing parametric investigations. Parametric studies involve the variation of each physical parameter individually to establish the effect of that physical parameter on the thermal response of the system. Thermal considerations in the design of food heating systems include the effects of the following physical quantities: (1) the thermophysical properties of the nutrient materials; (2) the power rating of the heater (i.e., the energy per unit surface area); (3) the control temperatures which activate the heating element; (4) the initial temperature of the nutrient material; and (5) the dimensions of the container. In the heat transfer field, the temperature is generally presented as a temperature difference ratio and time in dimensionless forms using Fourier modulus; however, the following results employ real time and temperature.

5.1 Effect of Thermophysical Properties

The thermophysical properties of the nutrient material have a substantial influence on the required heating time. In the conduction mechanism, the food must be able to conduct energy from near the heating surface to the center of the container. Of particular interest is the thermal diffusivity α which is the thermal conductivity divided by the product of the density and heat capacity (or specific heat) i.e., $\alpha = \frac{k}{\rho c}$. Rather than showing the temperature response of particular nutrient materials, the results are shown in terms of a ratio of thermal diffusivities (more specifically, the thermal diffusivity is normalized by dividing by the value for water at standard conditions). The response of the average temperature of the nutrient material is presented in Fig. 5.1a for the smaller container and Fig. 5.1b

Fig. 5.1a: Effect of Variation in Food Properties
(Small Container)

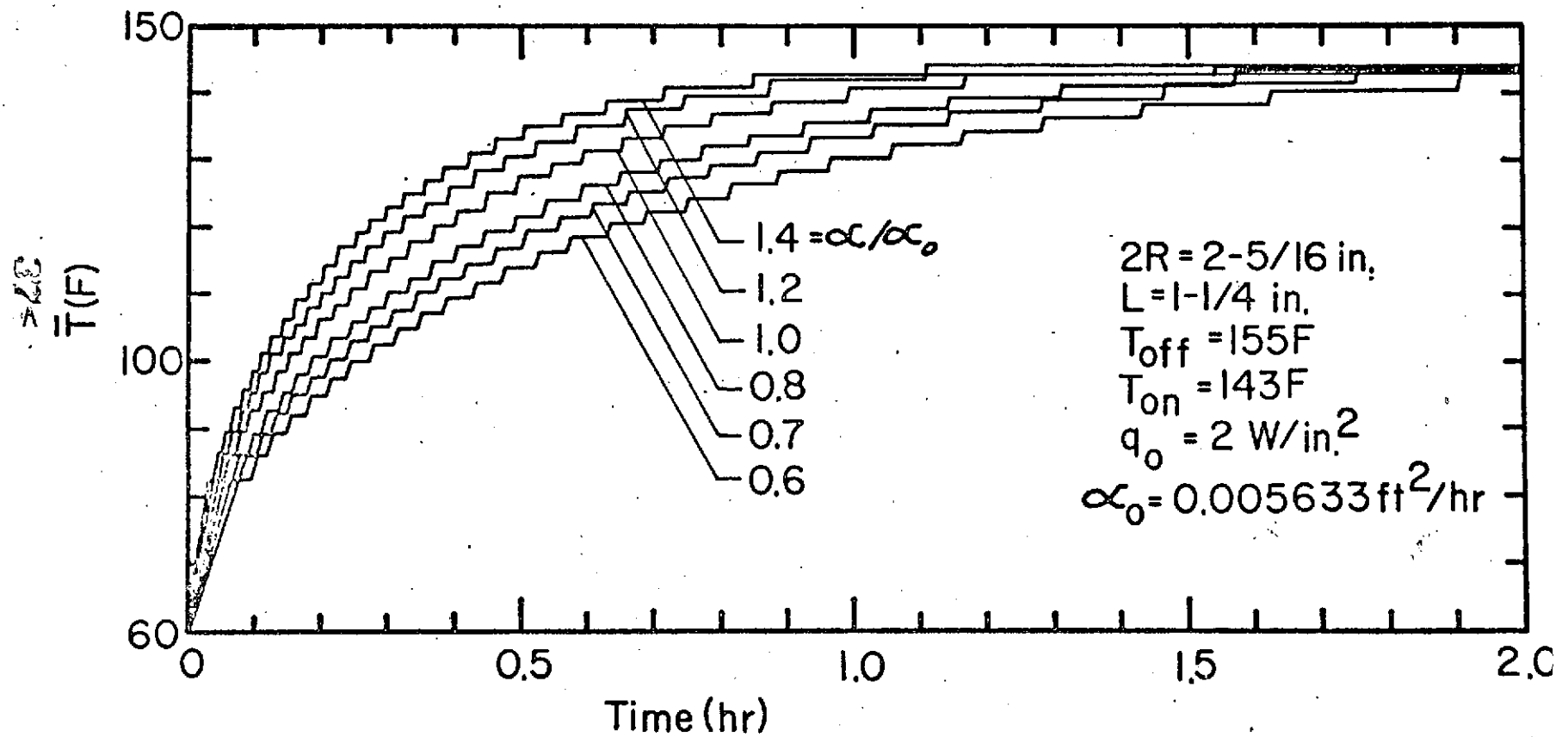
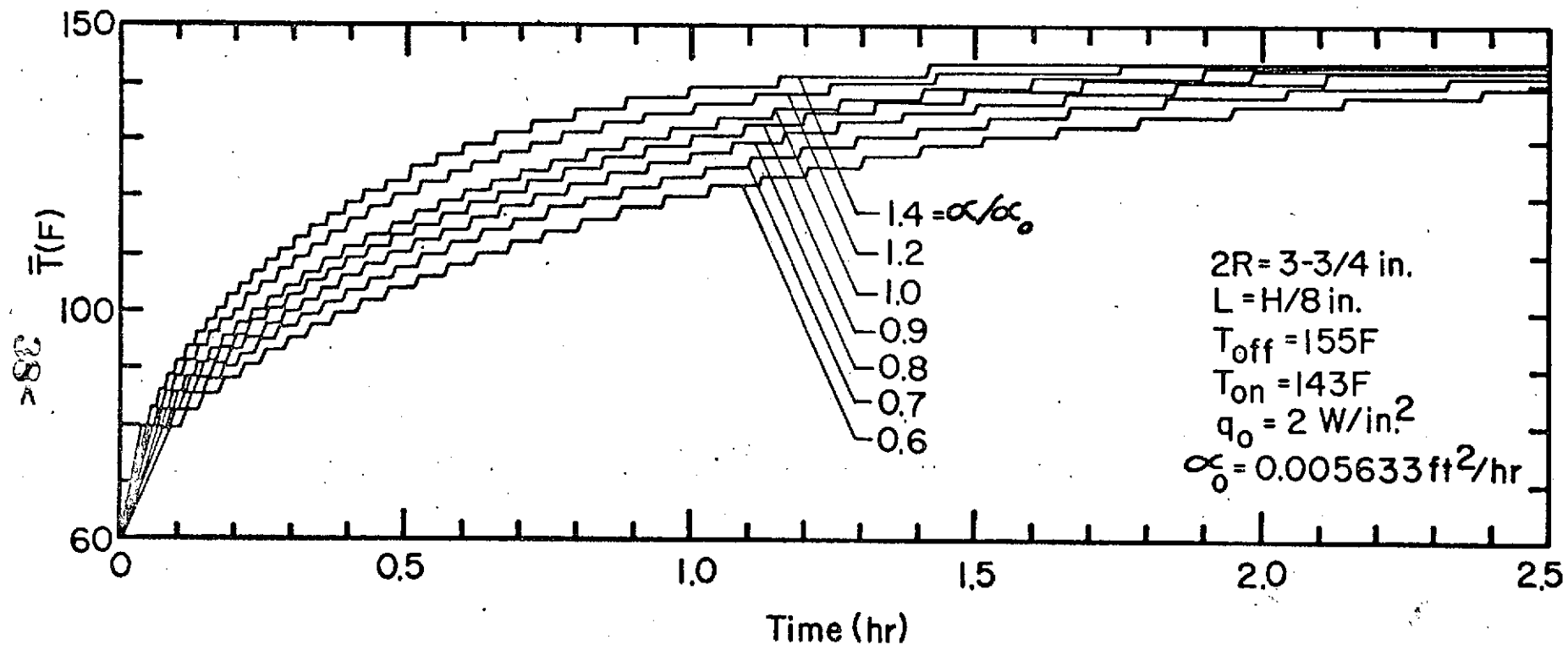


Fig. 5.1b: Effect of Variation in Food Properties (Large Container)



for the larger container.

5.2 Effect of Heater Output

If a nutrient material is heated by a uniform heat source which is not controlled, the heater would remain activated continuously until the desired average temperature of the food had been attained. However, if the nutrient material near the heating surfaces is not to experience excessive local temperatures, a control mechanism must be included in the heater circuit. The temperature-time relationships for the temperature controlled heater are compared to the uncontrolled heater in Fig. 5.2a for the small container and Fig. 5.2b for the larger container. The average and "coldspot" temperatures are depicted.

If the heater were continuously activated, a decrease in the heater output by one-half would increase the heating time (to a particular temperature) by two. However, when a temperature-controlled heater is employed, this effect is altered substantially. The effect of a variation in the surface heat flux is demonstrated in Fig. 5.3 for the small container when the initial temperature is 70F. The interesting point is that when the uniform surface heat flux is reduced by a factor of 8 from two (2) watts per square inch down to one-fourth ($\frac{1}{4}$) watts per square inch, the heating time did not increase by a factor anywhere near 8. For example, the nutrient material was heated from 70F to 130F in 0.62 hr for the high surface heat flux case and in 1.07 hr for the low surface heat flux case. In this situation when the surface heat flux was decreased by a factor of 8, the heating time was not even doubled. In optimizing a heating system for nutrient materials, the output of the surface heater is an important consideration. The reason the lower surface heat flux does not require a proportionally longer period of time is that the heater remains activated a substantially longer period of time prior to the initiation of a

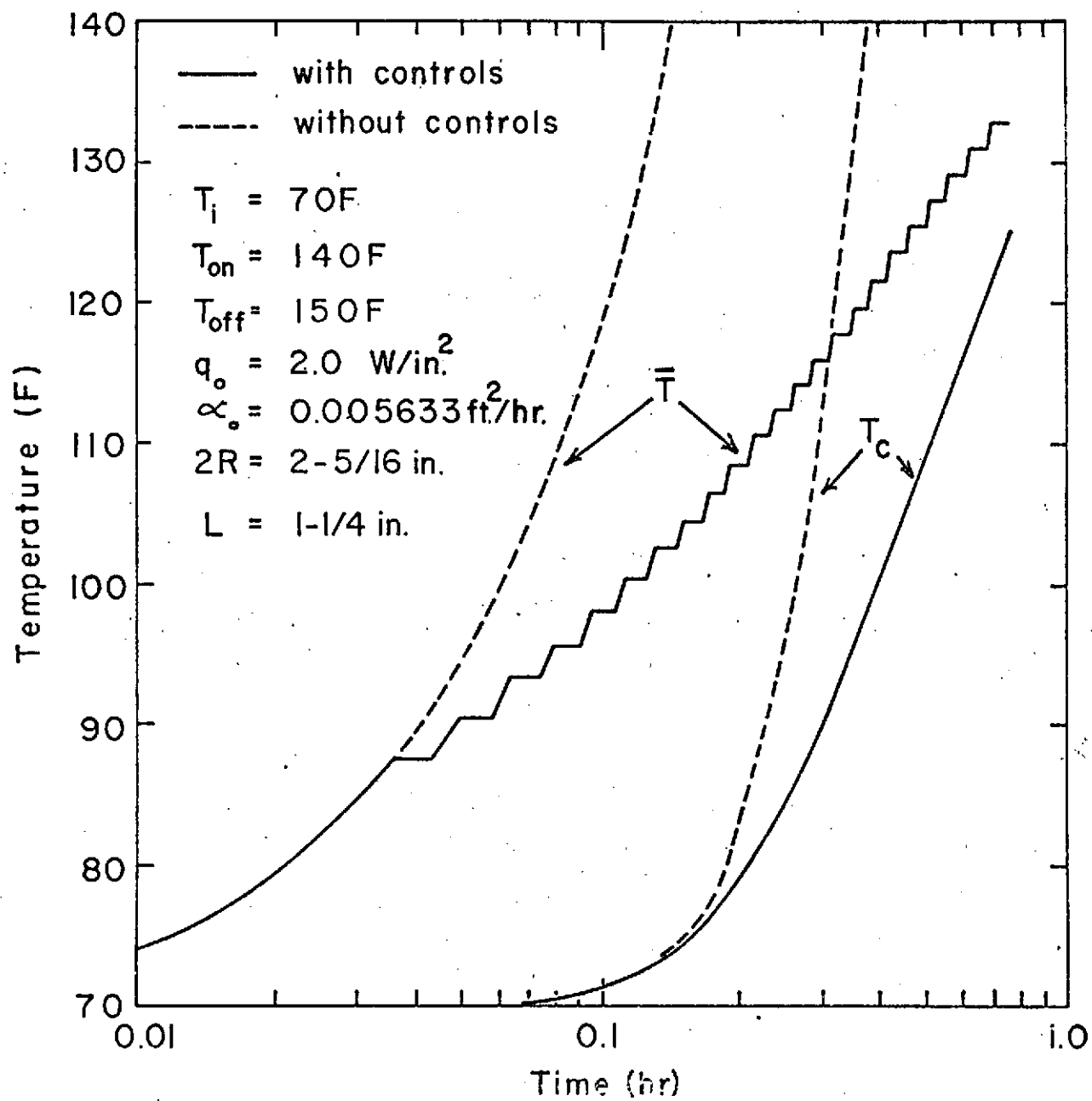


Fig. 5.2a: Comparison of Thermally Controlled Heater
with a Constant Continuous Heater
(Small Container)

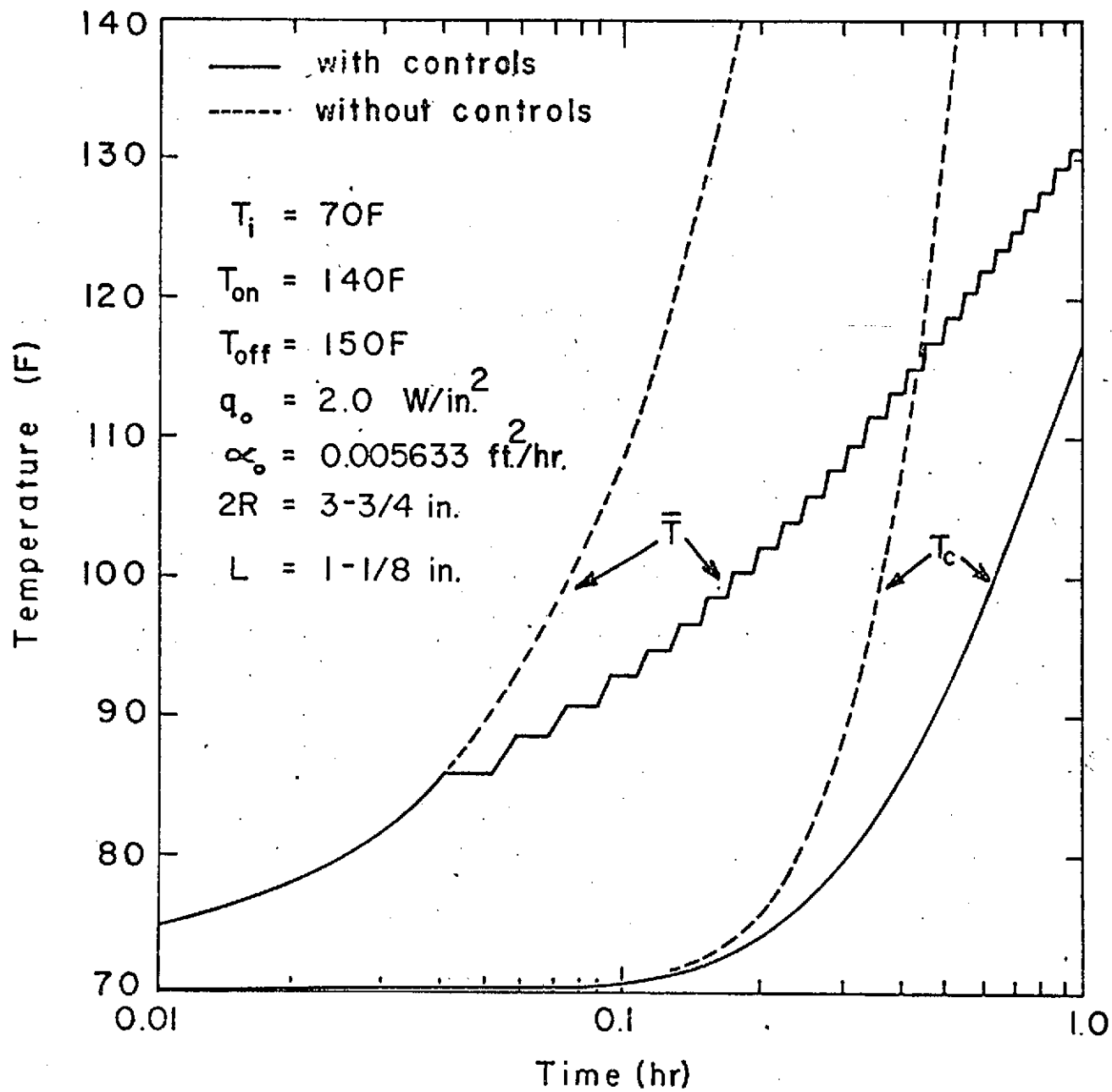
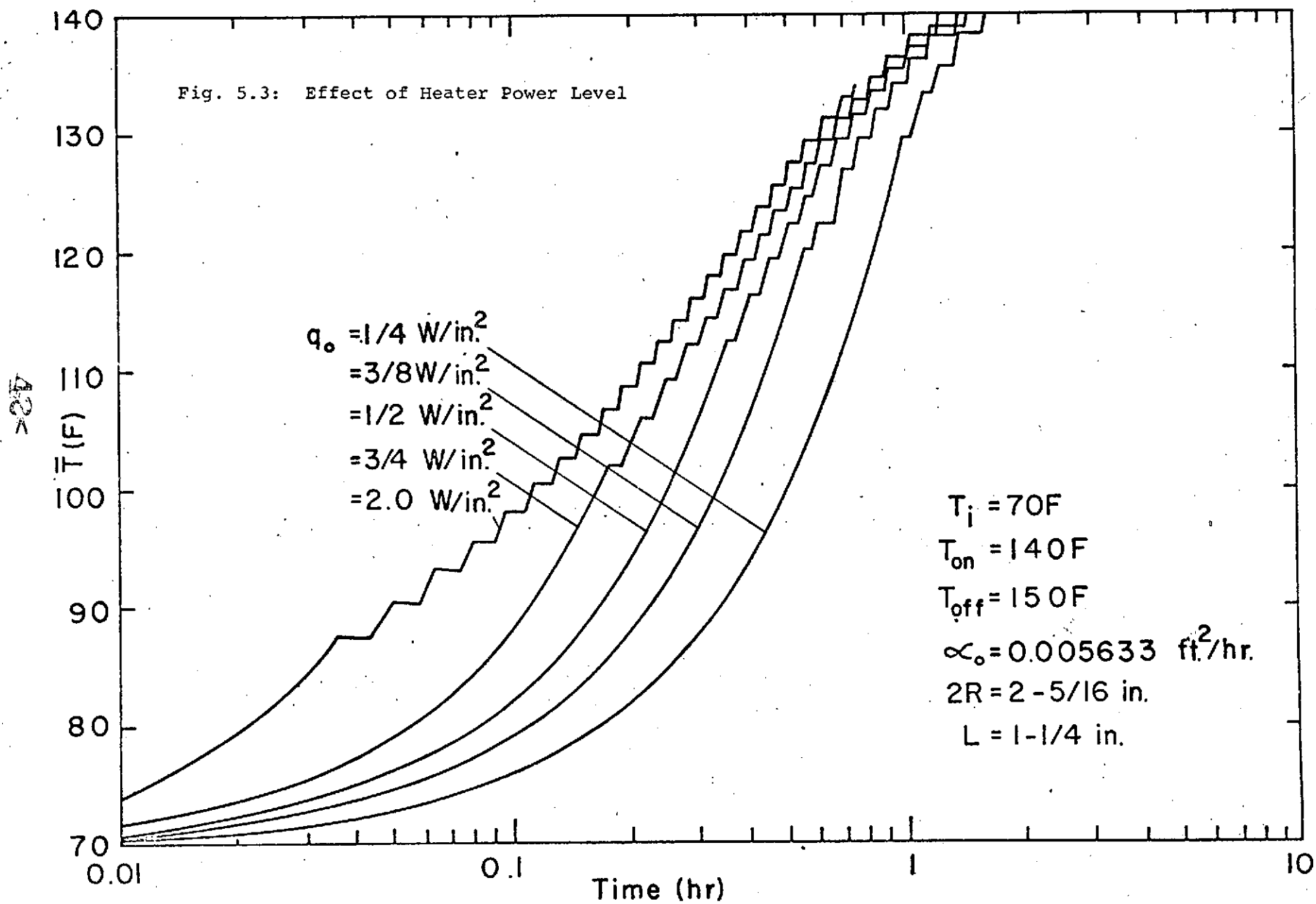


Fig. 5.2b: Comparison of Thermally Controlled Heater
 with a Constant Continuous Heater
 (Large Container)



periodic heater action. For the case of the higher surface heat flux, the heater begins its cycling pattern early.

5.3 Effect of Temperature Controls

The level of the temperature controls on the uniform surface heater has a great influence on the required heating times for the nutrient materials since the longer the heater cycling process can be delayed, the shorter the required heating time. Although the Skylab system has established the temperature control range of the heater, an investigation of the control levels can provide insight into the operational characteristics of the system.

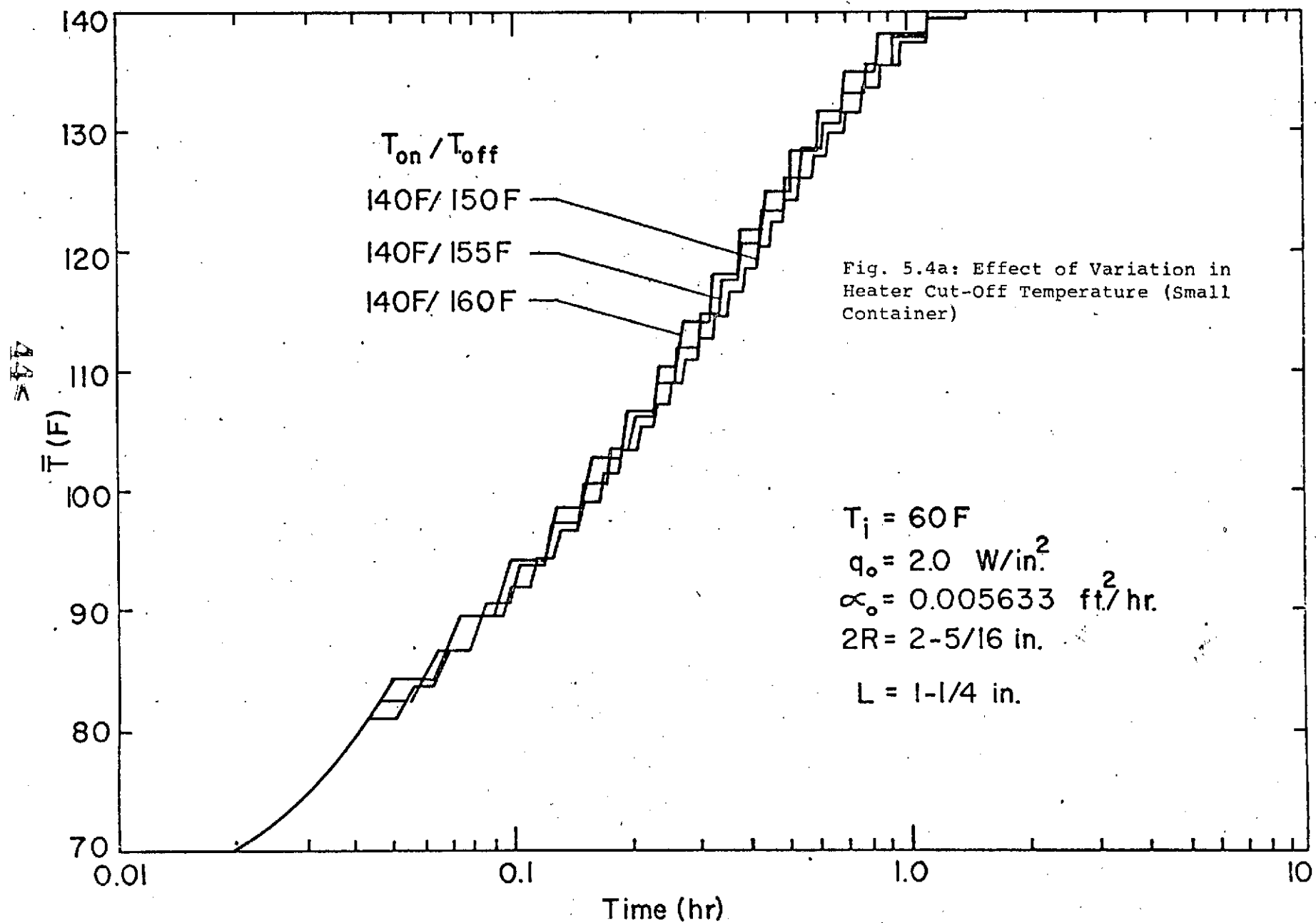
In studying the effect of the thermal control of the surface heater, two temperatures are considered - the surface temperature at which the heater is cut off and the surface temperature at which the heater is reactivated. In the model of the cylindrical container for the Skylab system, the point affected greatest by the surface heaters is the lower corner; the lower corner is the intersection of the bottom heated surface with the curved-side heated surface which corresponds to the location $r = R$, $z = 0$ in the model (Fig. 4.2). It is this point in the model which is used for the thermal control of the heater. Three situations are considered for each size container:

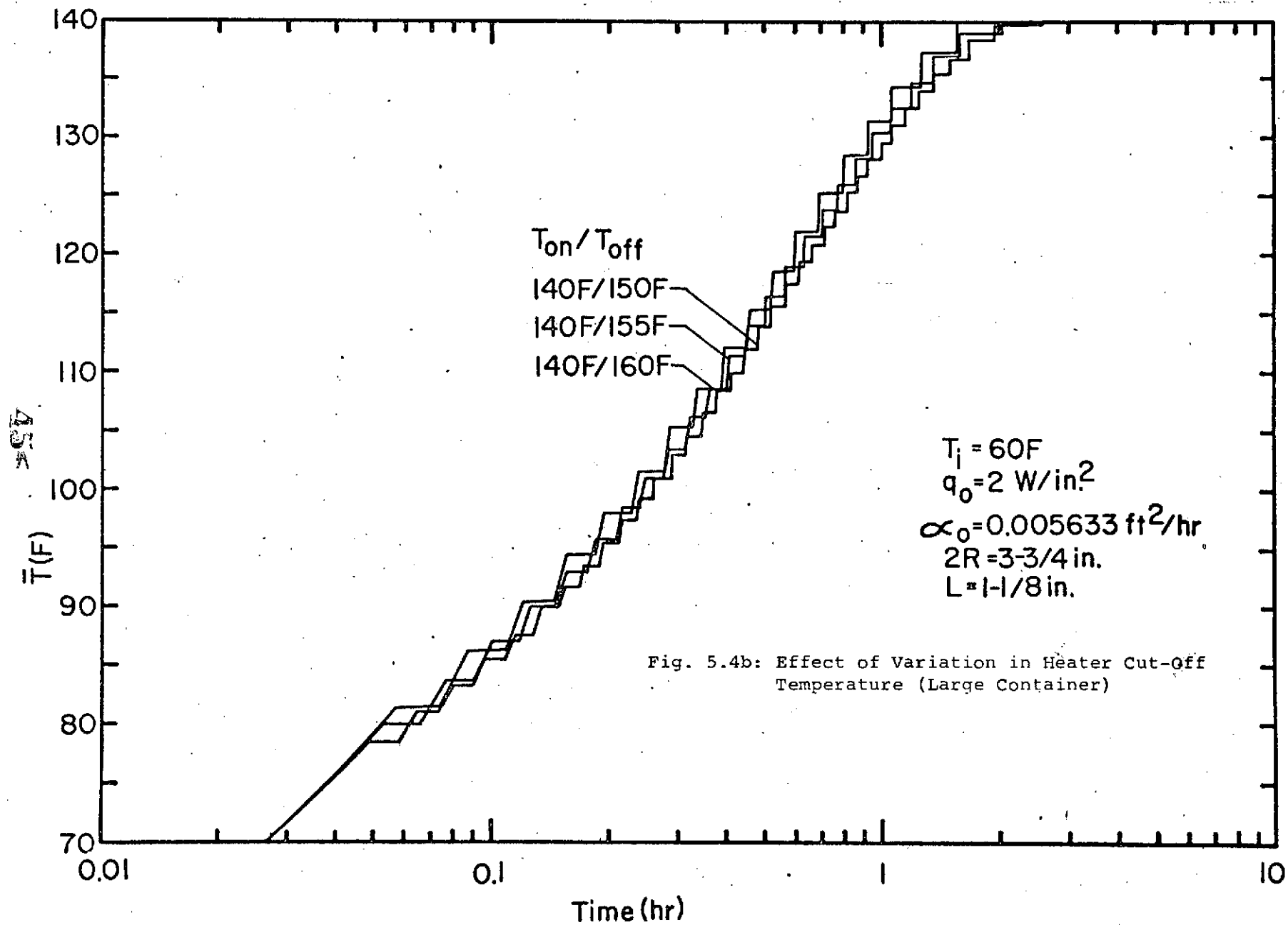
(a) Variation of the heater cut-off temperature (150F, 155F and 160F for a given heater cut-on temperature (140F) as shown in Fig. 5.4.

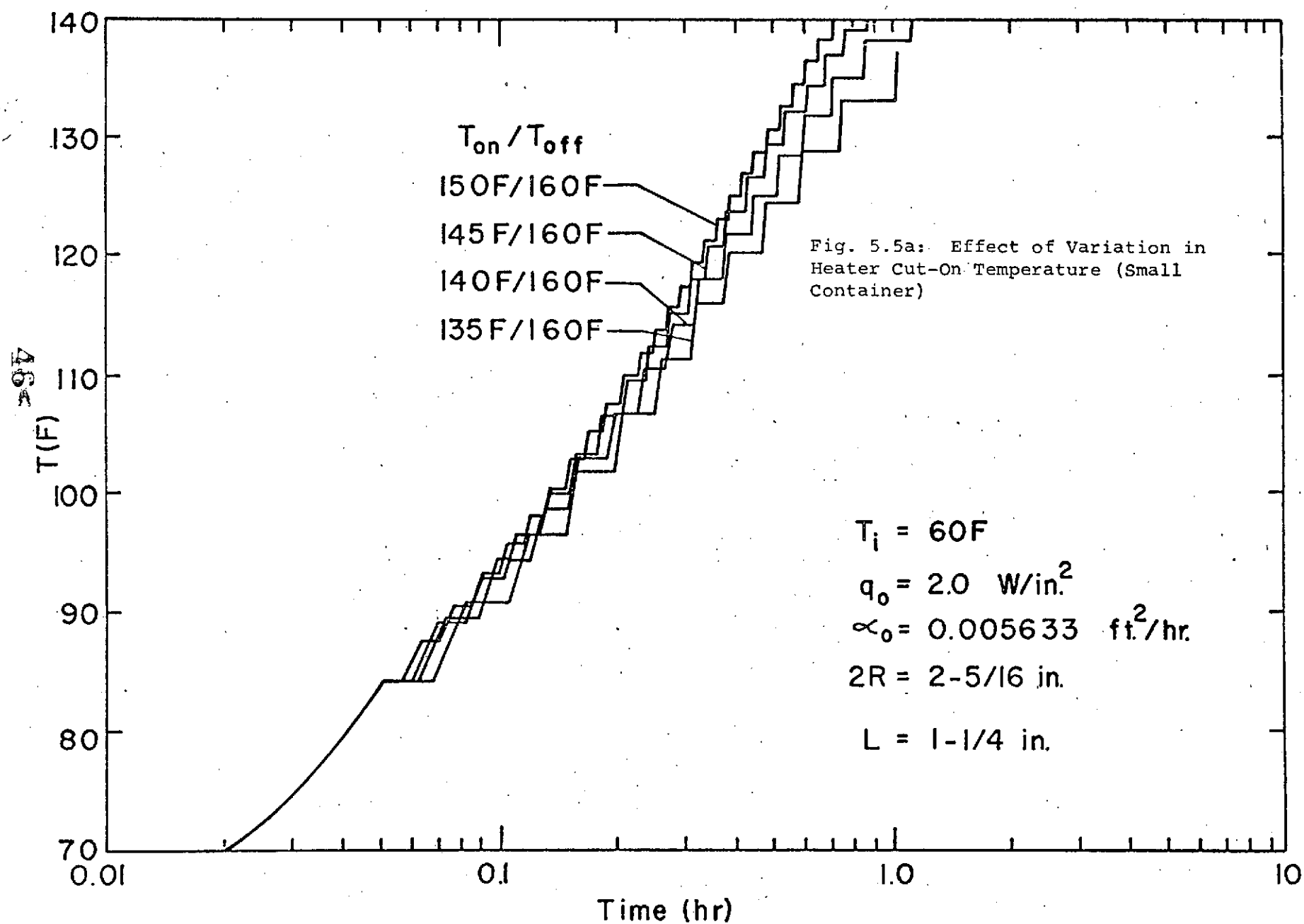
(b) Variation of the heater cut-on temperature (135F, 140F, 145F and 150F) for a given heater cut-off temperature (160F) as shown in Fig. 5.5.

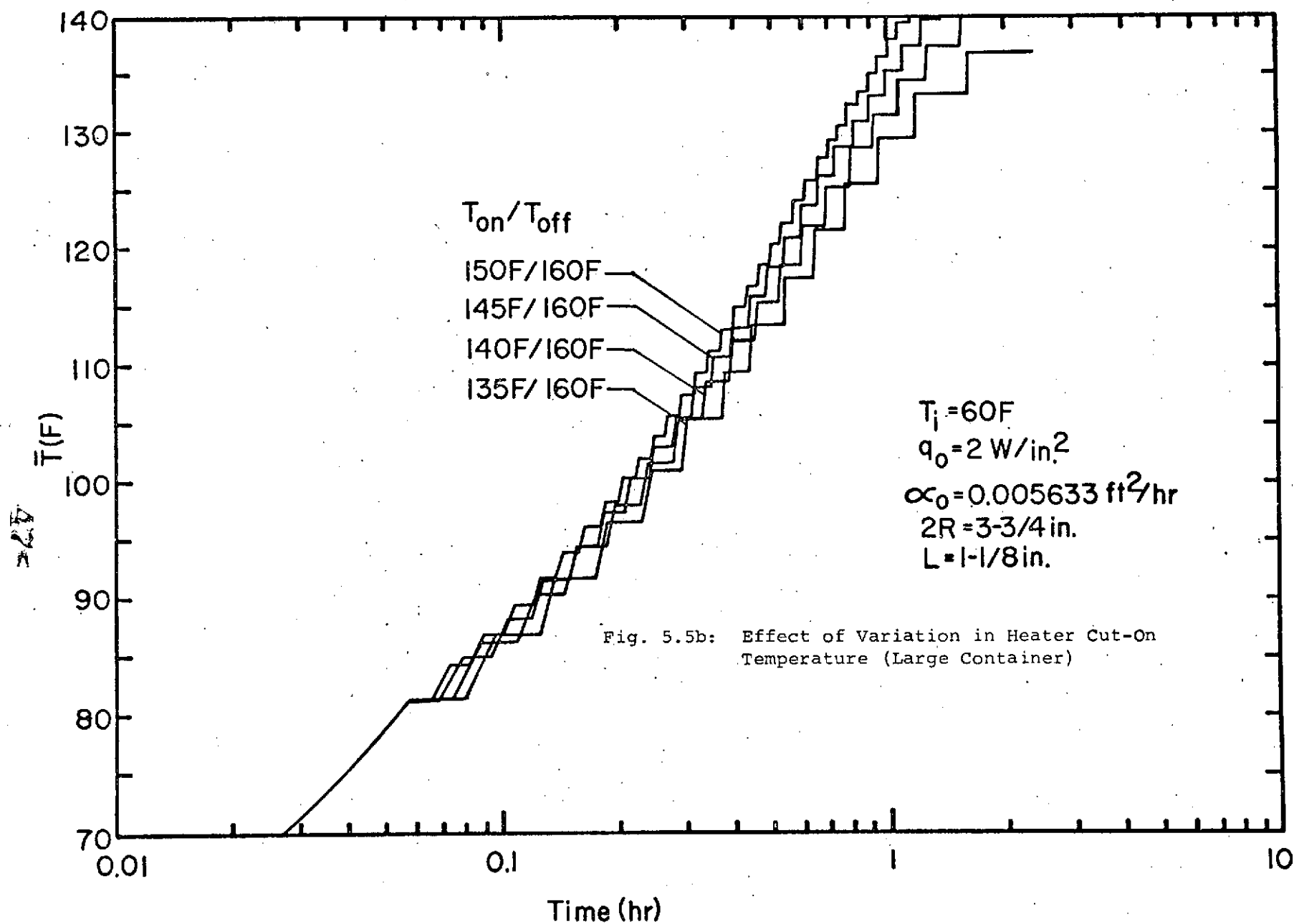
(c) Variation in the level of temperature control for a specified temperature difference $T_{\text{off}} - T_{\text{on}}$ (10F) as shown in Fig. 5.6.

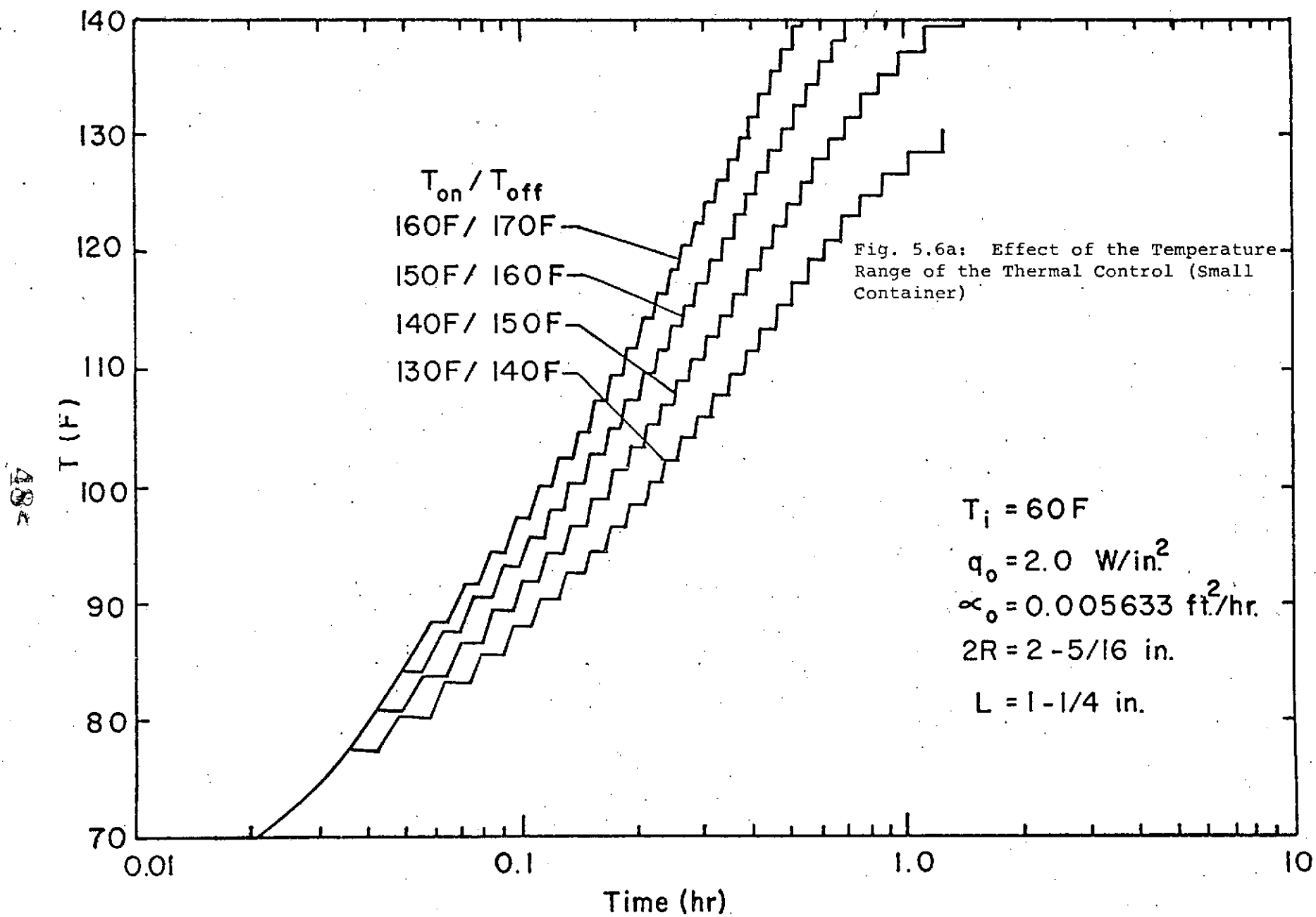
In comparing the 6 figures, the most significant effect on

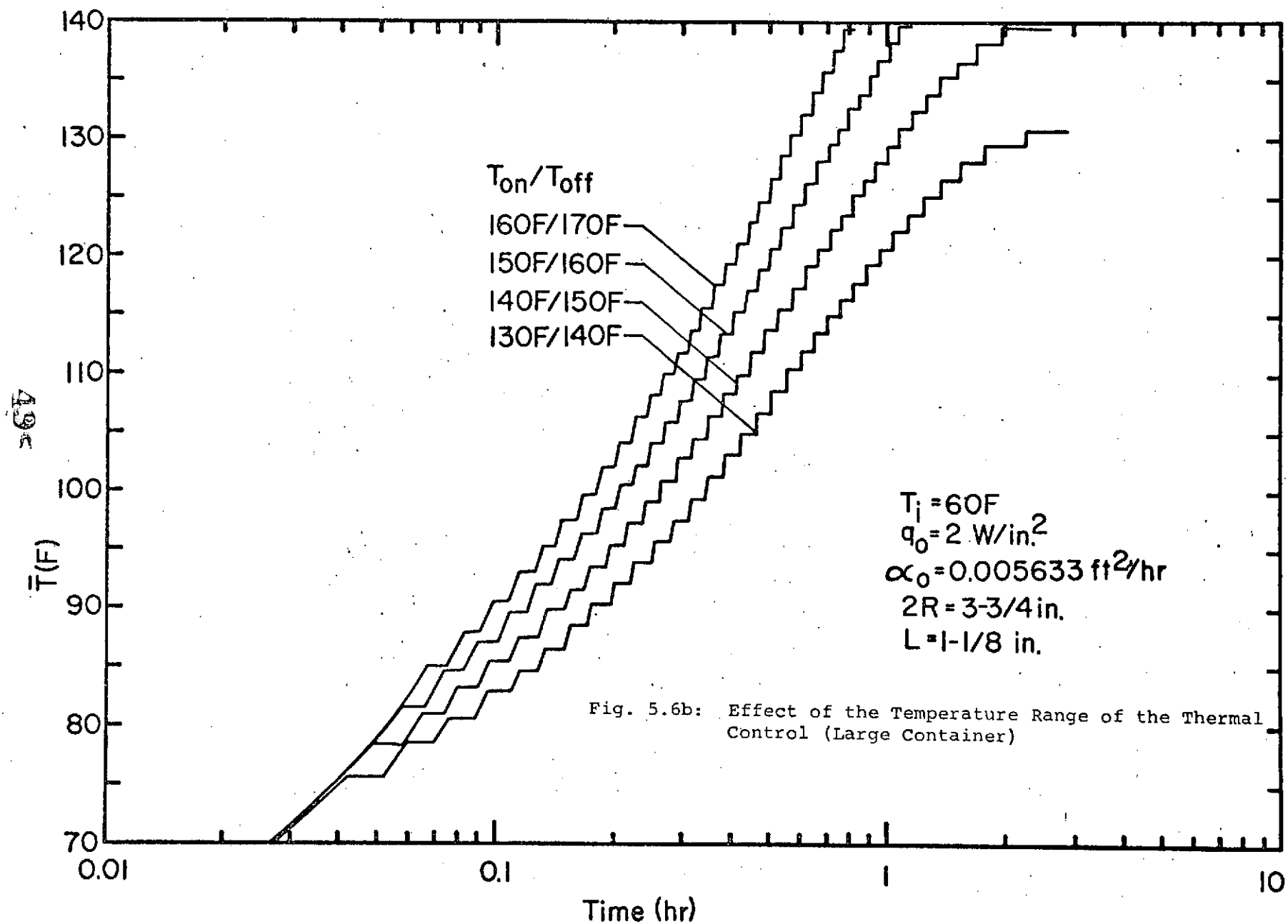












the heating times occurs when a constant temperature difference $T_{\text{off}} - T_{\text{on}}$ is maintained, permitting the range of the thermal control to change.

5.4 Effect of Initial Temperature

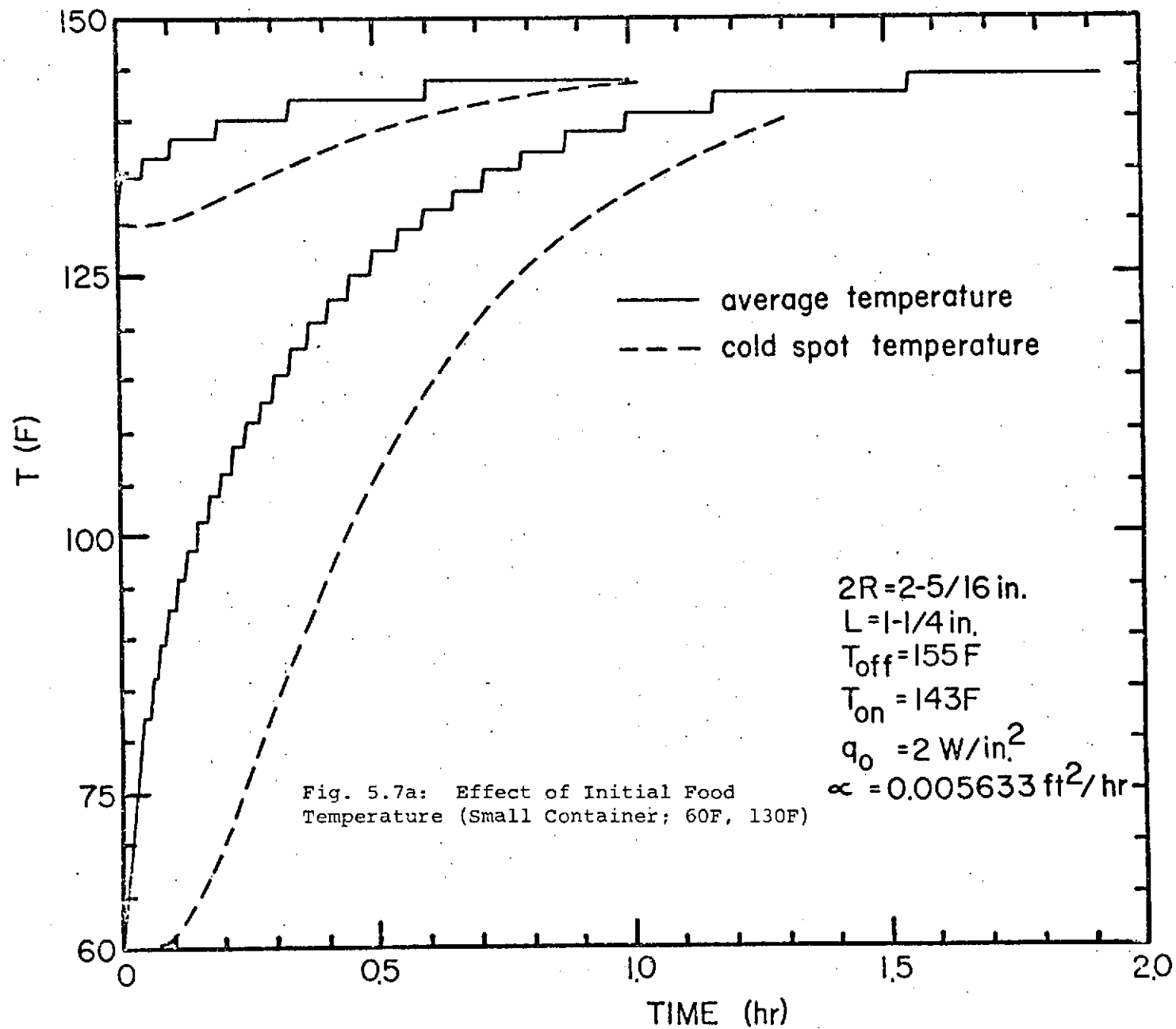
The initial temperature of the nutrient material is the most influential factor on heating-time requirements. Three initial temperatures of food substances are involved, namely 130F, 60F, and -10F. The thermal response of each container is shown in Fig. 5.7a and 5.7b for the 60F and 130F initial conditions. The thermal response of each container for an initial remperature of -10F is shown in Fig. 5.7c. It should be noted that the predictions shown in Fig. 5.7c do not include the energy of melting associated with the ordinary "thawing" process. The inclusion of the phase change increases the heating-time requirement.

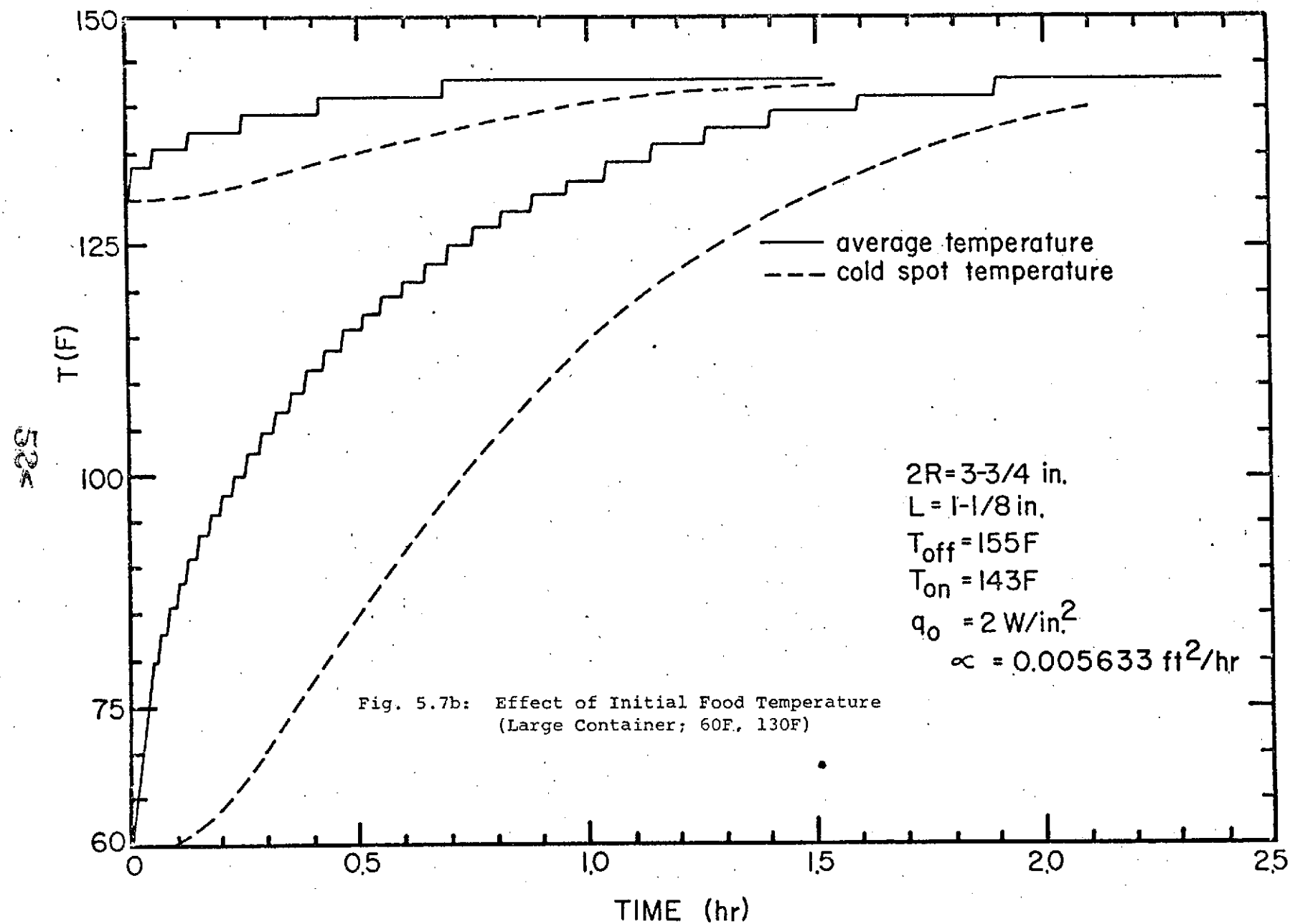
5.5 Effect of Container Size

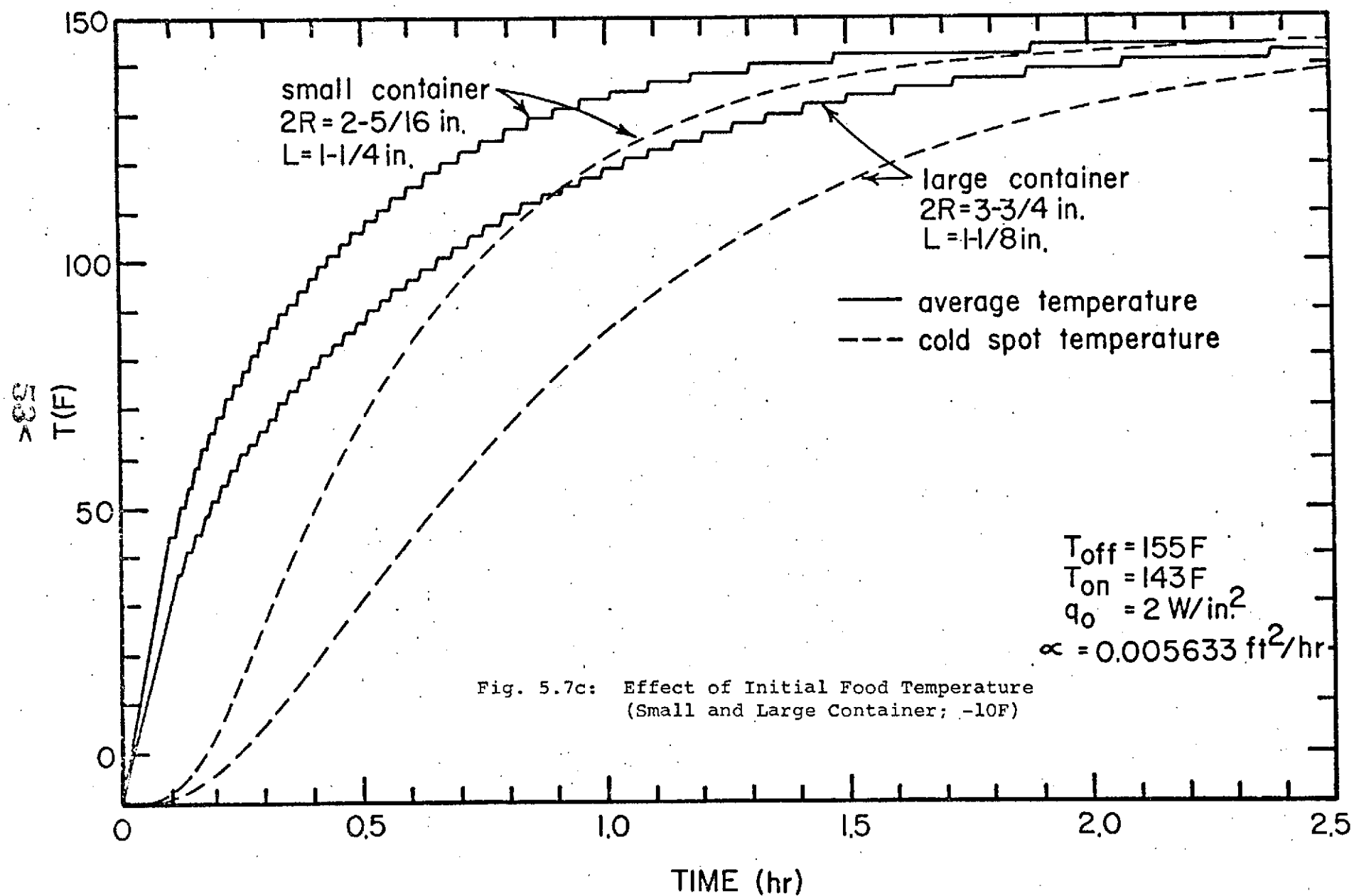
Since the size of the containers has already been established only the two container sizes to be used in the heating tray are included. Typical response characteristics are shown in Fig. 5.7c. Parametric studies could be performed to establish the effect of length-to-diameter ratios for the cylinder. It is desirable during the heating process to have the maximum heat transfer surface area per given volume of food. For a cylindrical container heated on the sides and bottom this size parameter, the ratio of heated surface area to volume, is

$$\Phi = \frac{\pi R^2 + 2\pi RL}{\pi R^2 L} = \frac{1}{L} + \frac{2}{R} \quad (5-1)$$

For the containers used in this study, the smaller container has a 30% larger size parameter, indicating that the heating is approximately 30% faster. This rough estimate is verified in Fig. 5.7c.







5.6 Discussion

The parameters involved in the parametric investigations were (1) thermal diffusivity of the nutrient material, (2) power rating of the heater, (3) control temperatures, (4) initial systems temperature, and (5) container dimensions.

A $\pm 40\%$ change in thermal diffusivity caused a $+4$ to -10°F change in the average temperature after 1 hour for the smaller container. Also a -0.4 to $+0.8$ hr delay in achieving the minimum required average temperature of 140°F resulted. The most interesting result (Fig. 5.3) shows that a reduction in heat flux by a factor of 8 increases heating time only marginally.

The effect of independently varying the lower or upper heater control temperature (Fig. 5.4 and 5.5) have only a small effect on heating time. However, as expected, adjusting the level of the control while keeping the difference between the upper and lower temperatures constant has considerable effect (Fig. 5.6).

The effect of initial temperature is qualitatively predictable. The lower the initial temperature, the longer the time required to heat the nutrient material. The significantly longer time required to heat "frozen" foods could represent a problem.

The above results can be summarized to show the effect of initial temperature, normalized thermal diffusivity, and the size parameter, respectively. Figure 5.8 indicates the time required for the average temperature to reach 140°F when the various parameters are varied independently from the standard configuration.

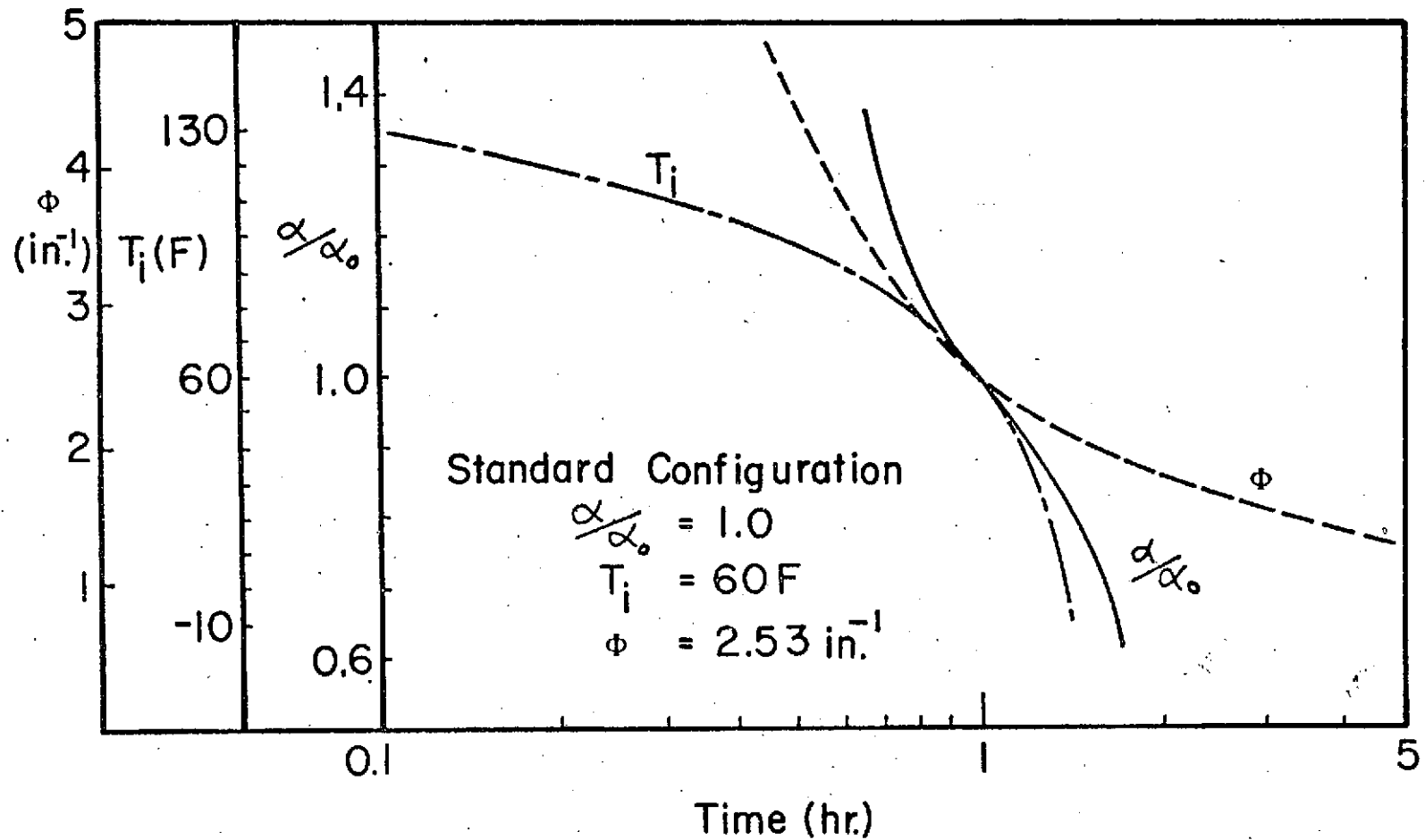


Fig. 5.8: Time for the Average Food Temperature to Reach 140F When the Normalized Thermal Diffusivity α/α_0 , Initial Temperature T_i , and Size Parameter Φ are varied from the Standard Configuration ($q_0=2 \text{ W/in}^2$, $T_{on}/T_{off}=143/155F$)

REFERENCES

1. Carslaw, H. S. and J. C. Jaeger, Conduction of Heat in Solids, 2nd Edition, Oxford (Clarendon) 1959.
2. Luikov, A. V., Analytical Heat Diffusion Theory, Academic Press, 1968.
3. Ölcer, N. Y., "On the Theory of Conduction Heat Transfer in Regions with Boundary Conditions of the Second Kind," International Journal of Heat and Mass Transfer, 8: 529-56, 1965.
4. Mathias, M. R., "A Study of the Effects of Cyclic (on-off) Heat Fluxes on Canned Food Heating Times During Skylab Space Flights," M.S. Thesis, University of Houston, 1972.
5. Ames, W. F., Numerical Methods for Partial Differential Equations, Barnes and Noble, Inc., 1969.
6. Forsythe, G. E. and W. R. Wasow, Finite-difference Methods for Partial Differential Equations, John Wiley and Sons, Inc., 1960.
7. Crandall, S. H., Engineering Analysis, McGraw-Hill Book Co., 1956.
8. Kreith, F., Principles of Heat Transfer, International Textbook Co., 1965.
9. Wiley, C. R., Jr., Advanced Engineering Mathematics, McGraw-Hill, 1960.

APPENDIX A

ADAPTATION OF ÖLÇER'S SOLUTION TO REQUIRED SOLUTION

Ölcer [3] solves the problem of the unsteady temperature distribution in a right circular solid cylinder of finite length with its entire surface subjected to boundary conditions of the second kind (heat flux). The three-dimensional transient solution has the form (quantities are defined in nomenclature and following):

$$\begin{aligned}
 T(r, \varphi, z, t) = & \frac{1}{\pi R^2 L} \int_{-\frac{L}{2}}^{\frac{L}{2}} \int_0^{2\pi} \int_0^R T_i(r, \varphi', z) r dr d\varphi dz \\
 & + \sum_{j=0}^3 \left[\Omega_j(t) + T_{0j}(r, \varphi, z, t) \right] \\
 & + \frac{2}{\pi R^2 L} \sum_{\ell=0}^{\infty} \sum_{m=0}^{\infty} \sum_{n=0}^{\infty} \frac{J_{\ell}(\mu_{\ell m} r) \cos\left(\frac{n\pi}{2} + \frac{n\pi z}{L}\right) \exp(-\alpha \lambda_{\ell mn}^2 t)}{(1 + \delta_{\ell 0})(1 + \delta_{n0}) \left[1 - \left(\frac{\ell}{\mu_{\ell m} R}\right)^2\right] J_{\ell}^2(\mu_{\ell m} R)} \\
 & \int_0^{2\pi} \left\{ \int_{-\frac{L}{2}}^{\frac{L}{2}} \int_0^R J_{\ell}(\mu_{\ell m} r) \cos\left(\frac{n\pi}{2} + \frac{n\pi z}{L}\right) \left[T_i(r, \varphi', z) - \frac{q''(r, \varphi', 0)}{k \lambda_{\ell mn}^2} \right] r dr dz \right. \\
 & - \frac{1}{k \lambda_{\ell mn}^2} \int_0^R J_{\ell}(\mu_{\ell m} r) \left[F_1(r, \varphi', 0) + (-1)^n F_2(r, \varphi', 0) \right] r dr \\
 & - \frac{R J_{\ell}(\mu_{\ell m} R)}{k \lambda_{\ell mn}^2} \int_{-\frac{L}{2}}^{\frac{L}{2}} \cos\left(\frac{n\pi}{2} + \frac{n\pi z}{L}\right) F_3(\varphi', z, 0) dz \\
 & \left. - \frac{1}{k \lambda_{\ell mn}^2} \int_0^t \exp(-\alpha \lambda_{\ell mn}^2 t) [\text{functions of } \dot{q}'', \dot{F}_1, \dot{F}_2, \dot{F}_3] dt \right\} \cos \ell(\varphi - \varphi') d
 \end{aligned} \tag{A-1}$$

where

F_1, F_2, F_3 are the fluxes at the bottom, top, and radial surfaces, respectively.

q'' is the internal heat source function.

The dot notation ($\dot{}$) indicates the derivative with respect to time.

The eigenvalues, λ_{lmn} , are given by

$$\lambda_{lmn}^2 = \mu_{lm}^2 + \left(\frac{n\pi}{L}\right)^2$$

where $\mu_{lm} R \geq 0$ is the n th root of

$$J'_l(\mu_{lm} R) = 0$$

and the prime ($'$) denotes differentiation with respect to the argument.

Also,

$$\Omega_0(t) = \frac{1}{\pi R^2 L} \frac{\alpha}{k} \int_0^t \int_{-\frac{L}{2}}^{\frac{L}{2}} \int_0^{2\pi} \int_0^R q''(r, \varphi, z, t) r dr d\varphi dz dt$$

$$\Omega_1(t) = \frac{1}{\pi R^2 L} \frac{\alpha}{k} \int_0^t \int_0^{2\pi} \int_0^R F_1(r, \varphi, t) r dr d\varphi dt$$

$$\Omega_2(t) = \frac{1}{\pi R^2 L} \frac{\alpha}{k} \int_0^t \int_0^{2\pi} \int_0^R F_2(r, \varphi, t) r dr d\varphi dt$$

$$\Omega_3(t) = \frac{1}{\pi R L} \frac{\alpha}{k} \int_0^t \int_{-\frac{L}{2}}^{\frac{L}{2}} \int_0^{2\pi} F_3(\varphi, z, t) d\varphi dz dt$$

and

$$T_{00}(r, \varphi, z, t) = f_n(Q) = 0$$

$$T_{01}(r, \varphi, z, t) = \text{fn}(F_1) = T_{01}(z, t) = \frac{2F_1}{Lk} \left[\frac{\left(\frac{L}{2} - z\right)^2}{4} - \frac{L^2}{12} \right]$$

$$T_{02}(r, \varphi, z, t) = \text{fn}(F_2) = T_{02}(z, t) = \frac{2F_2}{Lk} \left[\frac{\left(\frac{L}{2} + z\right)^2}{4} - \frac{L^2}{12} \right]$$

$$T_{03}(r, \varphi, z, t) = \text{fn}(F_3) = T_{03}(r, t) = \frac{RF_3}{2k} \left[\frac{r^2}{R^2} - \frac{1}{2} \right]$$

where axial symmetry implies

$$F_1 \neq \text{fn}(r)$$

$$F_2 \neq \text{fn}(r)$$

$$F_3 \neq \text{fn}(z)$$

In particular, for the heating of food

$$F_2 = 0$$

$$F_1 = F_3 = \begin{cases} q_0 & \text{heater on} \\ 0 & \text{heater off} \end{cases}$$

$$T_i(r, \varphi, z) = T_i(r, z)$$

and for axial symmetry $l = 0$. Therefore

$$\Omega_0 = 0$$

$$\Omega_1 = \frac{\alpha t}{kL} F_1$$

$$\Omega_2 = 0$$

$$\Omega_3 = \frac{2\alpha t}{kR} F_3$$

Equation (A.1) now becomes

$$\begin{aligned}
T(r, z, t) = & \frac{2}{R^2 L} \int_0^R \int_{-\frac{L}{2}}^{\frac{L}{2}} T_i(r, z) r dr dz \\
& + \left[\frac{\alpha t}{kL} + \frac{2\alpha t}{kR} \right] \left\{ \begin{matrix} q_0 \\ 0 \end{matrix} \right\} + \left[\frac{2}{kL} \left(\frac{\left(\frac{L}{2} - z \right)^2}{4} - \frac{L^2}{12} \right) + \frac{R}{2k} \left(\frac{r^2}{R^2} - \frac{1}{2} \right) \right] \left\{ \begin{matrix} q_0 \\ 0 \end{matrix} \right\} \\
& + \frac{16\pi}{R^2 L} \sum_{m=0}^{\infty} \sum_{n=0}^{\infty} \frac{J_0(\mu_m r) \cos\left(\frac{n\pi}{2} + \frac{n\pi z}{L}\right) \exp(-\alpha \lambda_{mn}^2 t)}{2(1 + \delta_{n0}) J_0^2(\mu_m R)} \\
& \left[\int_{-\frac{L}{2}}^{\frac{L}{2}} \int_0^R J_0(\mu_m r) \cos\left(\frac{n\pi}{2} + \frac{n\pi z}{L}\right) T_i(r, z) r dr dz \right. \\
& - \frac{1}{k \lambda_{mn}^2} \int_0^R J_0(\mu_m r) \left\{ \begin{matrix} q_0 \\ 0 \end{matrix} \right\} r dr \\
& \left. - \frac{R J_0(\mu_m R)}{k \lambda_{mn}^2} \int_{-\frac{L}{2}}^{\frac{L}{2}} \cos\left(\frac{n\pi}{2} + \frac{n\pi z}{L}\right) \left\{ \begin{matrix} q_0 \\ 0 \end{matrix} \right\} dz \right] \tag{A-2}
\end{aligned}$$

It is noted that

$$\begin{aligned}
\int_{-\frac{L}{2}}^{\frac{L}{2}} \cos\left(\frac{n\pi}{2} + \frac{n\pi z}{L}\right) dz &= \int_{-\frac{L}{2}}^{\frac{L}{2}} \left(\cos \frac{n\pi}{2} \cos \frac{n\pi z}{L} - \sin \frac{n\pi}{2} \sin \frac{n\pi z}{L} \right) dz \\
&= \frac{2L}{n\pi} \cos \frac{n\pi}{2} \sin \frac{n\pi}{2} \\
&= 0 \tag{A-3}
\end{aligned}$$

Since [9]

$$\frac{d}{dx} [x^v J_v(x)] = x^v J_{v-1}(x)$$

so that for $v = 1$

$$\frac{d}{dx} [x J_1(x)] = x J_0(x)$$

then

$$\begin{aligned} \int_0^R r J_0(\mu_m r) dr &= \frac{1}{\mu_m^2} \int_0^{\mu_m R} x J_0(x) dx \\ &= \frac{1}{\mu_m^2} \int_0^{\mu_m R} \frac{d}{dx} [x J_1(x)] dx \\ &= \frac{R}{\mu_m} J_1(\mu_m R) \end{aligned} \quad (A-4)$$

When Equations (A-2), (A-3), and (A-4) are combined:

$$\begin{aligned} T(r, z, t) &= \frac{2}{R^2 L} \int_{-\frac{L}{2}}^{\frac{L}{2}} \int_0^R T_i(r, z) r dr dz \\ &+ \left(\frac{\alpha t}{kL} + \frac{2\alpha t}{kR} \right) \{q_0\} \\ &+ \left[\frac{2}{kL} \left(\frac{\left(\frac{L}{2} - z\right)^2}{4} - \frac{L^2}{12} \right) + \frac{R}{2k} \left(\frac{r^2}{R^2} - \frac{1}{2} \right) \right] \{q_0\} \\ &+ \frac{16\pi}{R^2 L} \sum_{m=0}^{\infty} \sum_{n=0}^{\infty} \frac{J_0(\mu_m r) \cos\left(\frac{n\pi}{2} + \frac{n\pi z}{L}\right) \exp(-\alpha \lambda_{mn}^2 t)}{2(1 + \delta_{n0}) J_0^2(\mu_m R)} \\ &\left[\int_{-\frac{L}{2}}^{\frac{L}{2}} \int_0^R J_0(\mu_m r) \cos\left(\frac{n\pi}{2} + \frac{n\pi z}{L}\right) T_i(r, z) r dr dz \right. \\ &\left. - \frac{R J_1(\mu_m R)}{k \lambda_{mn} \mu_m} \{q_0\} \right] \end{aligned} \quad (A-5)$$

where

$$\lambda_{mn}^2 = \mu_m^2 + \left(\frac{n\pi}{L}\right)^2.$$

where

$\mu_m R \geq 0$ is the m th root of

$$J_0'(\mu_m R) = 0.$$

For the first heating period the initial temperature is uniform and

$$T_i(r, z) = T_i$$

so that the first integral is equal to T_i and the other integral involving T_i vanishes (by A-3).

APPENDIX B

COMPUTER PROGRAM DESCRIPTION FOR ANALYTICAL SOLUTION DISCUSSED IN SECTION 3.0

(For Infinite Cylinder)

The computer program has essentially four segments:

- a) Input and Initialization
- b) The Heating Phase
- c) The Insulated Phase
- d) Output

These four segments can be characterized as follows:

- a) Input and Initialization

The size (R) of the cylinder, the thermo-physical properties of the food (α, c, k), the heater flux (q_0), the initial temperature (T_i), the temperature ranges desired (T_{\min}, T_{\max}) and the time increment (Δt) are required data.

- b) The Heating Phase

The time is set to zero, then incremented until the wall (the hottest point) temperature reaches the maximum allowable temperature. Temperature distributions at selected times are stored as the cylinder heats. The final temperature distribution becomes the initial temperature distribution of the insulated phase.

- c) The Insulated Phase

The time is set to zero, then incremented until the wall temperature drops to the minimum temperature. Temperature distributions at selected times are stored as the wall temperature drops. The cold point temperature is checked to see if the food has been heated to the minimum temperature. The final temperature distribution becomes the initial temperature distribution of the next heating phase.

- d) Output

Desired temperature profiles, mean temperatures, cold spot temperatures, and hot spot temperatures are printed.

Figure B.1 is a simplified flow diagram of the computer program.

The letters to the right correspond to the phase described above.

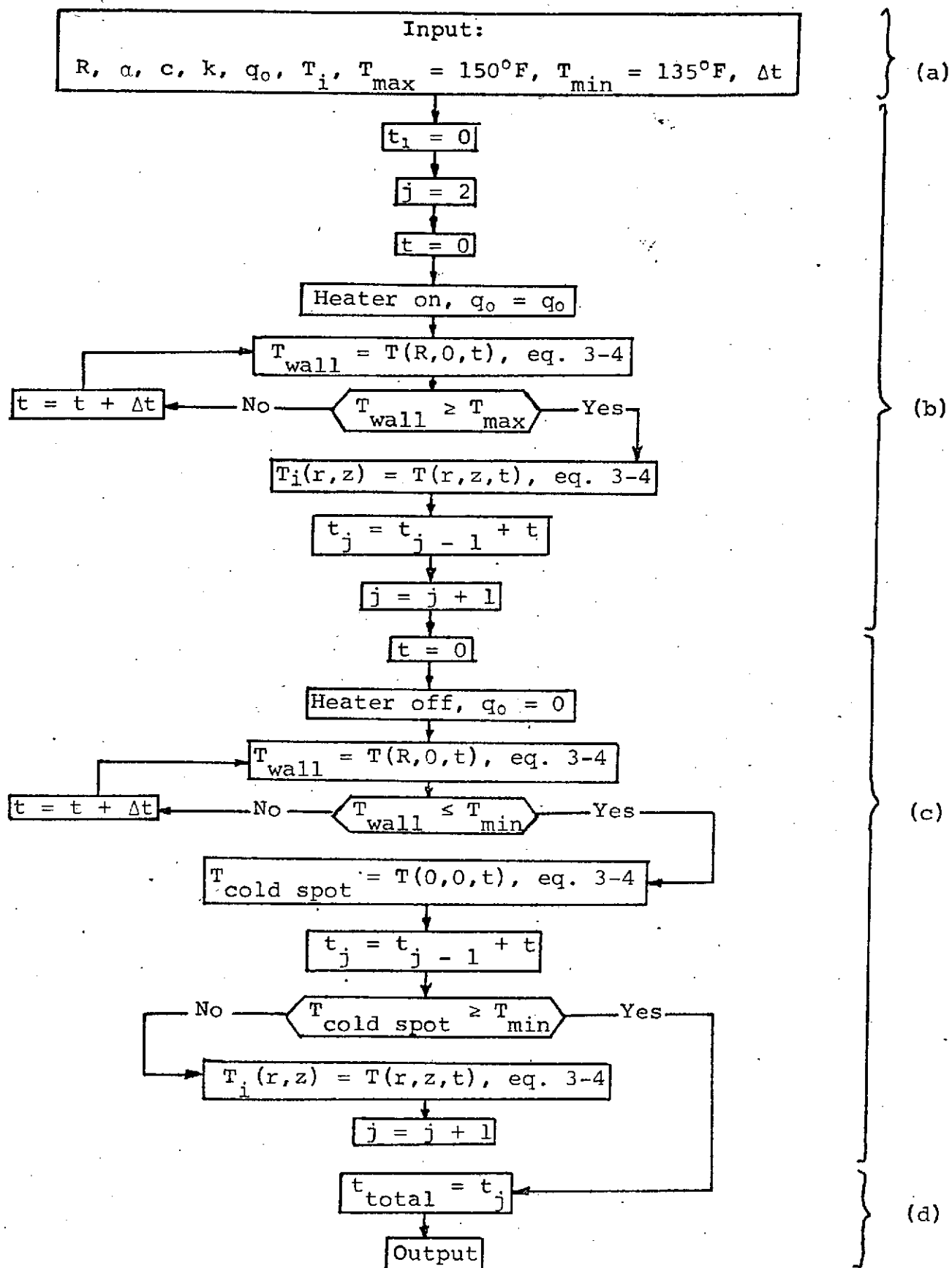


Figure B.1
Simplified Flow Chart

APPENDIX C

COMPUTER PROGRAM DESCRIPTION FOR NUMERICAL SOLUTION DISCUSSED IN SECTION 3.0

(Without Thawing)

The program follows closely the path outlined in Appendix B. Figure C.1 is a simplified flow diagram of the computer program.